UNIVERSIDADE FEDERAL DO RIO GRANDE DO SUL
INSTITUTO DE GEOCIÊNCIAS
PROGRAMA DE PÓS-GRADUAÇÃO EM GEOCIÊNCIAS

VARIAÇÃO ESPACIAL DA CARGA INTERFOLIAR DE ESMECTITAS DO DEPÓSITO DE BENTONITA DE MELO (NORTE DO URUGUAI). IMPLICAÇÕES NAS PROPRIEDADES FÍSICAS E NA ORGANOFILIZAÇÃO.

GABRIEL G. MACHADO A.

ORIENTADOR – Prof. Dr. André Sampaio Mexias

BANCA EXAMINADORA

Prof. Dr. Milton Luiz Laquintinie Formoso– Instituto de Geociências, Universidade federal do Rio Grande do Sul

Profa. Dra. Marcia Elisa Boscato Gomes – Instituto de Geociências, Universidade federal do Rio Grande do Sul

Prof. Dr. Norberto Dani - Instituto de Geociências, Universidade Federal do Rio Grande do Sul

Dissertação de Mestrado apresentada como requisito parcial para a obtenção do Título de Mestre em Geociências.

Porto Alegre – 2012

“Este documento é dedicado à minha filha Sofia pois ela representa a minha força nas diversas atividades do Mestrado Internacional Avançado em Ciências das Argilas”

Agradecimentos:

Ao Instituto de Geociências da Universidade Federal do Rio Grande do Sul, pela oportunidade de realizar este mestrado em um excelente ambiente de trabalho, com todo o suporte humano e material para a pesquisa. Ao pessoal docente do curso de Geologia pela dedicação e paciência.

Resumo:

Para a modelização da distribuição espacial da carga interfoliar das esmectitas de Melo foram amostrados quatro perfis, sendo dois obtidos a partir de furos de sondagens e dois com amostras coletadas na frente da cava de exploração da ocorrência. Os perfis formam aproximadamente uma figura com a forma de um trapezoide isósceles possuindo uma mediana em torno de 100 m. Foi analisado um total de 21 amostras a partir dos perfis. A camada de bentonita na área estudada varia de 5 a 6 metros de espessura e no perfil localiza-se entre a camada de solo do topo e uma camada sotoposta de arenito de granulação media a grossa. A composição mineralógica observada em rocha total ao XRD mostra um aumento do conteúdo de esmectita com a profundidade, estimando-se uma proporção de 30% a 50% na profundidade de 1,5m e de 90 a 96% na profundidade de 7 a 8,3 m, variando muito pouco de um perfil em relação a outro, porém, mantendo a tendência de aumento da esmectita em profundidade. Identifica-se montmorilonitas dioctaedricas magnesianas com predomínio de Ca na posição trocável, seguido de quartzo, feldspatos (albita e K-felçdspato) e raramente identifica-se traços de ilita e zeolitas (heulandita-clinoptilolita). A composição química por XRF também é coerente com a tendência observada na mineralogia, com uma diminuição em profundidade do teor de SiO_2, K_2O, Na_2O indicativo de menos quartzo e feldspato e um aumento do MgO oriundo das substituições octaédricas da esmectita que também é responsável pela origem da carga interfoliar, Al_2O_3 da posição octaédrica das esmectitas, Fe_2O_3 supostamente octaédrico e CaO que entra no sistema para compensar o desequilíbrio elétrico das cargas.

A carga interfoliar foi estimada na fração <1 μm por dois métodos sendo que a distribuição espacial mostra uma tendência de aumentar na parte intermediária da camada com valores em torno de 0,56 e/huc, diminuindo em direção ao topo e em profundidade com valores variando entre 0,46 a 0,48 e/huc. Esta variação gradual é melhor observada nos difratogramas do que através do método de cálculo da carga interfoliar, que não possuem sensibilidade suficiente para identificar as pequenas variações. Entretanto, variações na posição e na forma do pico 001 da esmectita são evidencias significativas que permitem validar as conclusões. O cálculo da formula unitária da montmorilonita mostra uma carga interfoliar de origem octaédrica com uma distribuição heterogenia ao longo do perfil reforçada pela variação na sorção organofílica e no grau de expansão observado na montmorilonita.

A avaliação da capacidade de troca de cátions (CEC) utilizada no projeto foi validada com o método do acetado de amônio, sendo que os valores obtidos foram diretamente proporcionais a estimativa da carga interfoliar das amostras. Valores de CEC entre 110 moles/100gr de argila corresponde a uma carga interfoliar da ordem de 0,55 e/huc e valores em torno de 90 moles/100gr de argila correspondem a cargas interfoliares em torno de 0,46 e/huc. A quantidade de cloreto de dodecylammonium ($C_{12}H_{28}CIN$) utilisado para organofilização foi proporcional a media do CEC. Em relação às propriedades físicas e organofilização, os padrões dos difratogramas das argilas organofilicas mostraram uma tendência de expansibilidade em função da carga interfoliar e a posição do pico 001 da montmorilonita-($C_{12}H_{28}CIN$) que variou de 17,05Å a 17,68Å. Pode-se considerar como um complexo bicamadas organo argilas, classicamente esperadas a 17,46Å considerando o tamanho da cadeia alkyl utilizada e a isoterma de sorção conhecida. As pequenas variações são indicativas da presença de camadas não intercaladas devido a heterogeneidade da carga. Embora as pequenas diferenças no espaçamento “d” entre as amostras, a relação da 001 argila organofilica do perfil em função da carga interfoliar, apresentou uma correlação perfeita. Comparando no perfil, o espaçamento 001 da argila orgânica tende a aumentar com a carga intefoliar. A posição do pico 001 varia entre 17,15Å e 17,5Å e a área do pico 001 após a organofilização variou entre 2620,6 (cps x deg) até 418,8 (cps x deg).

A tendência observada para a distribuição espacial da carga interfoliar esta provavelmente relacionada com uma variação gradual da permeabilidade e da razão água/rocha durante a alteração. A zona media da camada que concentra os mais elevados valores de carga interfoliar mostrou frequentemente a presença de uma textura esferulítica. Também, traços de zeolitas no XRD foram encontrados somente em amostras da profundidade entre 4 e 6 metros, indicando que a razão água/rocha estava no limiar do campo de estabilidade onde as zeolitas são favorecidas em detrimento das esmectitas no processo alteração do vidro vulcânico.

Palavras-chave: Bentonita, montmorilonita, carga interfoliar, organofilização.

Abstract:

To model the spatial distribution of key smectite properties, four profiles were sampled, two coming from boreholes and 2 from fresh cut samples over the mining front, Forming roughly an Isosceles Trapezoid with a median of approximately 100 m; 21 samples were analyzed over the four profiles. Bentonite bed ranges in the studied area from 5 to 6 m thick underlying top soil layer and overlaying a gross grain sandstone layer. Mineralogical composition observed on whole rock XRD traces showed an increasing content of the smectitic phase as a function of depth, going from 30% to 50% at around 1,5 m depth to 90 to 96 % at a depth ranging 7 to 8,3 m depth, varying very slightly from one profile to another but keeping the trend. Mayor mineral phases identified were Mg rich dioctahedral montmorillonite with mainly Ca in exchangeable position, Quartz, feldspar (Albite and K-feldspar) and only occasionally as trace phases we observed Illite and Zeolites (heulandite-clinoptilolite). XRF chemical analysis results are also coherent with this vertical tendencies, expressed in a notable decrease of a SiO_2, K_2O, Na_2O indicating less quartz and feldspar species; and with increasing of MgO as octahedral substitution representing the main source of layer charge, Al_2O_3 most octahedral but also in a rather small amount as tetrahedral substitutions, Fe_2O_3 presumably octahedral and CaO compensating electrical charge desequilibrium.

Layer charge was estimated on the <1 μm size fraction by two methods and spatial distribution shows a clear trend to increase at the middle of the bed up to values around 0,56 e/huc and decrease towards top and bottom over values ranging from 0.46 to 0,48 e/huc. This gradual variations can be better observed on the XRD patters than by actual layer charge calculation methods results, given the fact that for this slight variances, commonly used methods are not sensible enough, Nevertheless the 001 peak position and shape of the smectite phase represents sufficient evidence for conclusions. Layer charge distribution is mainly Octahedral derived from unit formula calculations and Layer charge is clearly heterogeneous due to Organophilic sorption and swelling behavior observed.

Cation exchange capacity was calculated by ammonium acetate method, values obtained are directly proportional to layer charge estimations over those samples. CEC values around 110 moles/100gr of clay correspond to Layer charge on the order of 0,55 e/huc and values around 90 moles/100gr of clay to layer charges around 0,46 e/huc. The amount of dodecylammonium Chloride ($C_{12}H_{28}CIN$) used for organophilization was established proportional to the CEC average. Regarding the implications on physical properties and organophilization, XRD patterns of Organophilic clays showed a tendency on expandability as a function of layer charge in terms of their 001 ($C_{12}H_{28}CIN$)-Montmorillonite peak position, ranging from 17,05 Å To 17,68 Å. They could all be considered as bilayer intercalated Organoclay complexes, classically expected at 17,46 Å according size of the alkyl chain used, and the known sorption isotherm. The slight variances are indicating the presence of non-intercalated sheets due to charge heterogeneity. Despite the slight d-spacing differences among samples, the relationship 001 Organophilic C profile as a function of layer charge has a perfect correlation. Comparing a single profile, 001 d-spacing of organoclays tends to increase with increasing layer charge. The position of the 001 peak ranges between 17.15 Å and 17.5 Å and the raw 001 peak area after organophilization can vary from 2620.6(cps x deg) to 418.8 (cps x deg).

The tendencies observed for layer charge spatial distribution are probably related to gradual variations of permeability and water/rock ratio during alteration, the middle zone of the bed that concentrates higher values of layer charge also has showed very frequent presence of spherulitic textures that may belonged originally of opal-CT but replaced by recrystallized quartz unlike top and bottom of the bed, also Zeolites XRD traces were only found in samples located from 4 to 6 m depth, indicating that water rock ratio close to the threshold where Zeolites are favored with respect to smectites as a product of alteration.

Keywords: Bentonite, montmorilonite, layer charge, organophilization

Sumário

Lista de Figuras

Sobre a estrutura desta dissertação:

Esta dissertação de Mestrado está estruturada em torno de um artigo submetido a um periódico nacional. Sua organização compreende as seguintes partes principais:

Introdução. Introdução ao tema, contendo descrição geral e objetivos.

Corpo principal: Dissertação elaborada com os dados do projeto denominada,

"VARIAÇÃO ESPACIAL DA CARGA INTERFOLIAR DE ESMECTITAS DO DEPÓSITO DE BENTONITA DE MELO (NORTE DO URUGUAI). IMPLICAÇÕES NAS PROPRIEDADES FÍSICAS E NA ORGANOFILIZAÇÃO"

1 - Introdução

Bentonita talvez seja a argila industrial mais utilizada devido as suas excepcionais propriedades. Por centenas de anos e ainda hoje a tecnologia tenta controlar os parâmetros chaves que determinam o comportamento das fases esmectitas que formam a bentonita, especialmente quando esta interage com outros tipos de compostos. Em especial quando a interação esta relacionada com a troca dos cátions intercamadas das esmectitas naturais, sendo este o caso em várias aplicações industriais, medicas e ambientais.

Interessante o fato que mesmo sendo a carga interfoliar reconhecida como uma, se não a mais importante propriedade da família das esmectitas e fundamental para a compreensão da capacidade de interação destes minerais, ainda existe uma lacuna no conhecimento da sua distribuição nas ocorrências de bentonita, da influencia dos processos diagenéticos e sobre os métodos apropriados para sua estimativa.

O depósito de bentonta de Melo, norte do Uruguai, tem sido descrito como praticamente uma argila monomineralica formada por esmectita cálcica dioctaedrica originária da alteração de cinza vulcânica riolítica, depositada em ambiente transicional lagunar durante o Permiano Superior. O contexto geológico dos estratos que contem a bentonita, associado a bacia sedimentar intracratônica do Paraná permitiram preservar a esmectita, que não apresenta sinais de ilitização apesar da idade.. Por outro lado a preservação da esmectita no tempo geológico transforma esta bentonita numa importante fonte para pesquisas no campo dos processos diagenéticos e também sobre a distribuição espacial das propriedades químicas e físicas.

As implicações industriais do conhecimento das variações da carga interfoliar é explorado neste projeto visando a organofilização de um conjunto de amostras selecionadas pelo critério da variação da carga interfoliar. Os resultados produziram informações sobre as relações entre a variação espacial da carga interfoliar e as propriedades de sorção das montmorilonitas.

O projeto atual foi desenvolvido como uma pesquisa em conjunto entre a Universidade Técnica de Creta e a Universidade Federal do Rio Grande do Sul, sob a

supervisão de George Christidis (TUC) e Prof. Norberto Dani (UFRGS). O resultado da pesquisa tem como objetivo elaborar um documento para ser apresentado como requisito parcial para a obtenção do Título de Mestre em Geociências da UFRGS e no Programa "Erasmus Mundus" intitulado "International Master in Advanced Clay Science" com o suporte financeiro da Clay Mineral Society (CMS).

2 – Generalidades

2.1 - Localização

As ocorrências de bentonita de Bañado de Medina, objeto deste estudo, estão localizadas a 20 Km na direção SW d cidade de Melo, na rodovia para Fraile Muerto, norte do Uruguai, como é mostrado na imagem de satélite (Figura 01).

Figura 1 – Localização geográfica das ocorrências de bentonita do Bañado de Medina.

A região onde se encontram as ocorrências de bentonita são utilizadas como fazendas para criação de gado possuindo uma fisiografia plana dentro do bioma denominado de "Pampa", muito característico do local. A área alvo para exploração da ocorrência tem alguns hectares e apenas uma pequena parte esta sendo utilizada como pode ser visualizado no mapa georreferenciado da figura 02.

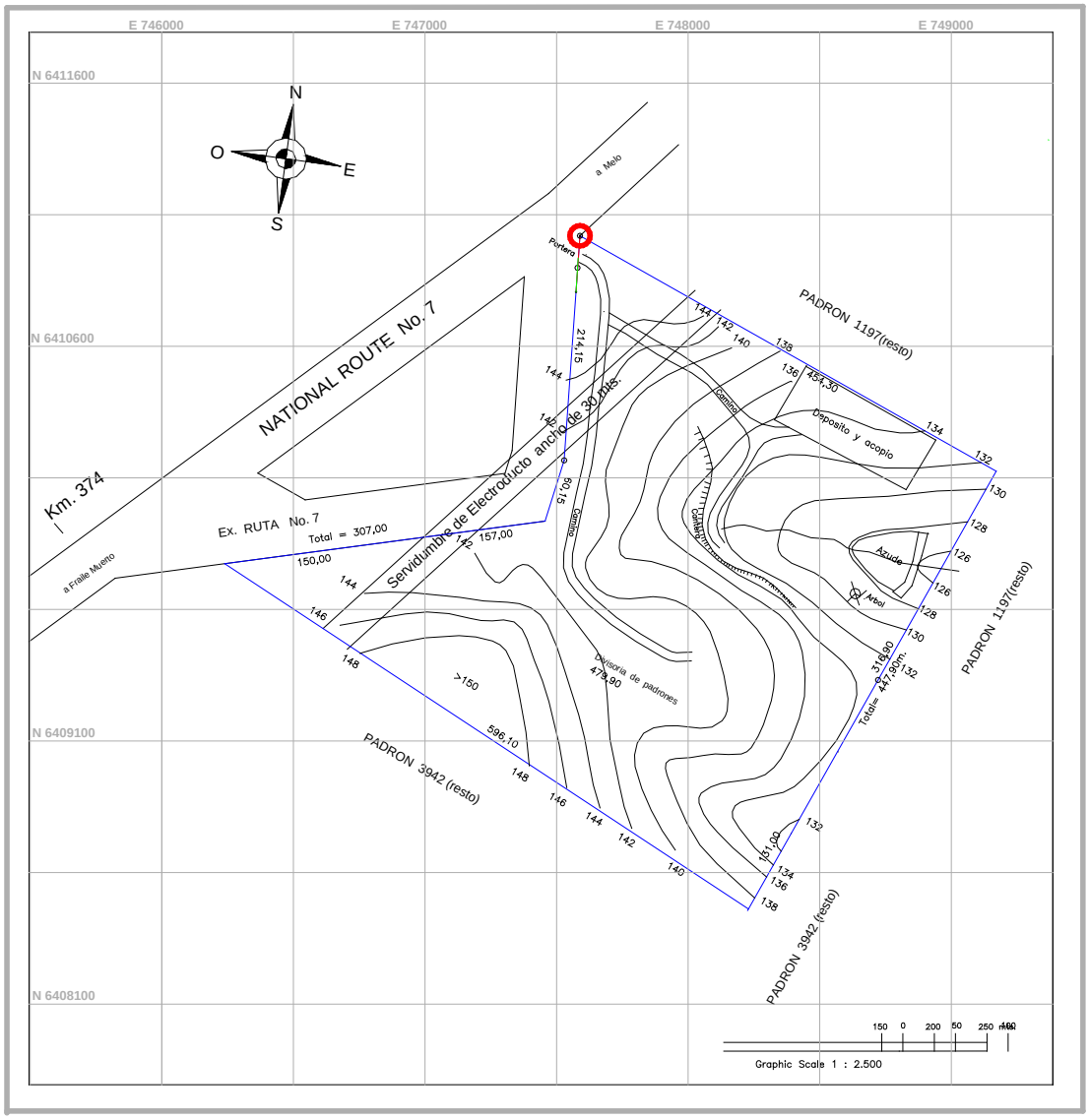

Figura 2- Mapa georreferenciado mostrando a localização da bentonita de Melo e detalhes da topografia (equidistância das curvas de nível de 1 metro).

2.2- Como acessar a ocorrência

A partir de Porto Alegre, Rio Grande do Sul, utiliza-se a BR290 por uma distância de 250 Km na direção oeste. Após acessa-se a BR473 até a cidade de Bagé na direção SW. Pela mesma rodovia chega-se a cidade de Aceguá, fronteiriça entre o Brasil e Uruguai. Continua-se par o sul pela Rodovia Nacional 8 por mais 60 Km até a cidade de Melo. Finalmente, para chegar a ocorrência de Bañado de Medina utiliza-se a Rodovia Nacional 7 na direção sudoeste por uma distância de 17 Km, quando então toma-se a Rodovia 26 que dará acesso a ocorrência a uma distância aproximada de 2 Km a esquerda da rodovia.

O polígono azul na figura 02 marca o perímetro da área de mineração e os limites da ocorrência de bentonita. O ponto em vermellho na figura 02 é uma referência utilizada pela empresa para fazer o levantamento detalhado da topografia, realizado com estação total.

2.3 – Contexto Geológico

A ocorrência de bontonita de Bañado de Medina localizada a 18 Km sudoeste da cidade Melo, norte do Uruguai, tem sido caracterizada e geologicamente descrita como uma argila essencialmente monominerálica constituída de esmectita dioctaedrica com Ca como o principal cátion trocável na posição intercamada (Calarge et al. 2001). Desenvolveu-se a partir da alteração de cinzas vulcânicas depositadas num ambiente transicional lagunar. Pertence estratigraficamente a Formação Rio do Rastro no Permiano Superior (equivalente a Formação Yaguari no Uruguai, Andreis et al. 1996, Rocha-Campos et al. 2010). Embora sendo uma ocorrência do Permiano, manteve-se preservada devido ao contexto geológico especial ligado a Bacia Intracratônica do Paraná e localmente devido a um grupo de falhas que protegeram camadas relativamente pouco espessas de bentonita da erosão. Representam uma importante fonte de informação para estudos envolvendo processo diageneticos e no estudo da variação de propriedades físicas e químicas em função da sua distribuição espacial.

A camada de bentonita de Bañado de Medina tem sido correlacionada com área fonte vulcânica de composição riolítica (Coutinho et al. 1981. 1991). A possível fonte vulcânica estaria localizada no sudoeste da Argentina. Formoso et al (1998) datou as camadas como Permiano Inferior a Médio. Caralge et al (2001) e Meunier et al (2005) correlacionam Bañado de Medina com as ocorrências de bontonita em Aceguá, sul do Brasil, baseado em similaridades mineralógicas e na assinatura química de minerais pesados e elementos terras raras (REE). Sugerem que a variação dos elementos maiores, RRE e abundancia dos elementos menores na camada de argila indicam dois eventos sucessivos de queda de cinzas vulcânicas. O teor dos elementos traços indicam um vidro vulcânico fracionado derivado de magmas riolíticos produzidos numa contexto geológico de subducção/colisão.

Com relação à fonte vulcânica, Rocha-Campos et al (2009) consideram que a província ígnea de Choiyoi do bloco São Rafael, localizado no oeste da Argentina (Patagônia) poderia ser considerada como a área fonte do vulcanismo durante o

Permiano. A figura 03 mostra a influencia geográfica deste vulcanismo. Embora Melo possui uma idade permiana, a atividade vulcânica do norte da Patagônia atingiu seu pico no Triássico e no Jurássico Inferior (Andreis et al, 1996), sendo eventos mais explosivos devido a natureza felsica dos magmas (Axelrod, 1985).

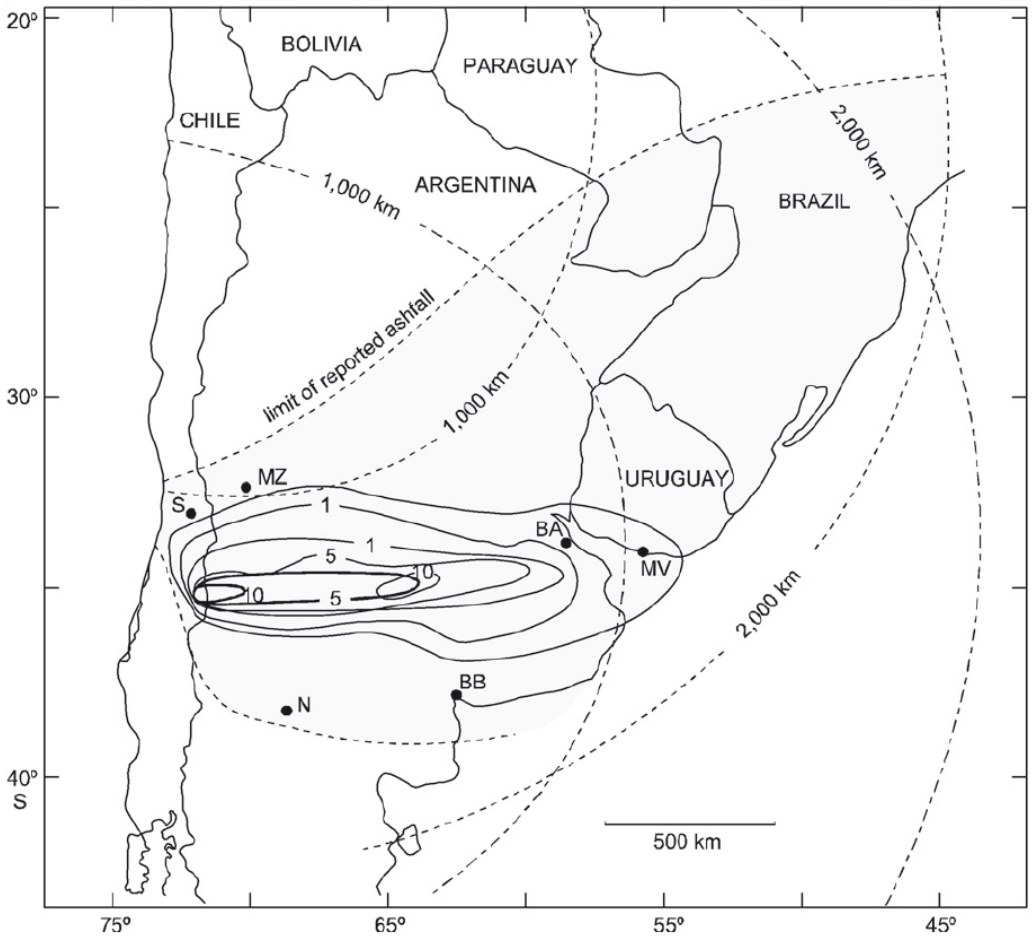

Figura 3 – Círculos com raios de 1000 e 2000 km centrados na área de São Rafael e nordeste da província ígnea Choyoi; Mapa base: distribuição de cinza vulcânica durante a erupção de Quiza Pu em 1932 (Hiltrech and Drake, 1992). Curvas de contorno mais espessas contendo as espessuras de cinza depositadas determinadas por Larsson (1937). MZ: Mendoza; BA: Buenos Aires; MV: Montevideo; S: Santiago, N: Neuquen; BB: Bahia Blanca. As erupções exemplificariam a dispersão da cinza vulcânica que cobriria distancias comparáveis com aquelas do Vulcanismo Choiyoi. (Rocha-Campos et al., 2009)

2.4 – Justificativas para a realização da pesquisa

A justificativa do projeto salientado anteriormente relaciona-se com a importância da distribuição espacial da carga interfoliar e suas implicações na

industrialização da bentonita. Entretanto outros aspectos da investigação devem ser mencionados:

1. Atualmente a pequena ocorrencia de Bañado de Medina esta explorado com metodos de escavação a céu aberto sem critérios de mistura ou de homogeneização das diferentes frentes. Cerca de 30% a 35% dos 9 m ou 7 m de um perfil tipico é descartado. Somente as seções com elevada proporção de esmectita são exploradas. A XRD mostra que em profundidades de 1,5 m – 2,2 m a partir da cobertura de solotem um conteudo siginificativo de montmorilonita dioctaedrica em proporções que podem variar entre 25% a 60%. Isto fica exemplificado nos perfis F1, C e F2. De acordo com o uso final a mistura de materiais com diferentes proporções de montmorilonita pode ser conveniente no sentido de extender as reservas e a vida util da ocorrência.
2. Os resultados da pesquisa podem servir como criterios de prospecção, considerando que a fonte vulcanica da bentonta esta localizada na Patagonia e foi ativa até o Jurásico Superior. A distância a partir da área fonte permite pensar na possibilidade de se encontrar ocorrencias similares com interesse economico numa ampla área. Camadas similares, embora com espessuras pequenas foram encontradas no sul do Brasil. O entendimento das condições diageneticas da ocorrência e as variáveis de preservação pode estabelecer parametros para prever outras ocurrencias. O entendimento de como a carga interfoliar do depósito vvaria e como afeta as propriedades física, será possivel predizer a qualidade outras ocorrências em relação ao processo diagenetico identificado.
3. A estimativa da carga interfoliar será feita por dois metodos diferentes (Christidis E. G. et al,. 2003), será possivel comparar os resultados em amostras com diferentes cargas intefoliares e proximo a margem de erro dos metodos.

3 – Resultados e conclusões

A carga interfoliar da esmectita na ocorrencia de Bañado de Medina tende a ser maior nas porçoes centrais da camada de bentonita. Para a utilização industrial da bentonita é importante o entendimento das substituiçoes octaédricas e tetraédricas na estrutura das escmectitas que irão se refletir nas propriedades no contexto das aplicações.

Observou-se uma correlação entre o padrão dos difratogramas das organoargilas ($C_{12}H_{28}CIN$)-montmorilonita com os valores da carga interfoliar. O espaçamento do pico 001 organoargila tende a aumentar com o aumento da carga interfoliar. O complexo argila com a amina tende a ser do tipo bicamada.

Os resultados também podem ser aplicados para estimar a quantidade de reagentes que deverão ser empregados para estimular a troca catiônica da esmectita. Aplicando-se o conhecimento da distribuição da carga interfoliar otimizaria o tratamento da esmectita e a metodologia de mistura de diferentes esmectitas encontradas ao longo do perfil.

Texto completo submetido à Universidade Técnica de Creta e para a Universidade Federal do Rio Grande do Sul

SPATIAL VARIATION OF LAYER CHARGE IN MELO BENTONITE DEPOSIT LOCATED IN NORTHERN URUGUAY. IMPLICATIONS ON PHYSICAL PROPERTIES AND ORGANOPHILIZATION

By:
Gabriel G. Machado A.

Supervised by:

Prof. Dr, George Christidis
&
Prof Dr, Norberto Dani

A thesis presented to the graduate schools of Technical University of Crete and Universidade Federal do Rio Grande do Sul as a requirement for the degree of International Master in Advanced Clay Science

Chania, Grece
2012

“This document is dedicated to my daughter Sofia, for she was the driven force
That made me succeed on the International Master in Advanced Clay Science”

TABLE OF CONTENT

LIST OF FIGURES

LIST OF TABLES

CHAPTER I

1.1 - Introduction

Bentonite have been perhaps one of the most widely use industrial clays due to their amazing physical properties, It has been the case for hundreds of years and yet we are still mastering the art of controlling key parameters that determine the behaviour of smectite phases within bentonites, when interacting to any other kind of compounds. Particularly when this interaction is related to the exchangeability of interlayer cations on natural smectite, and it is broadly the case in Industrial, medical, environmental and other applications.

It is indeed remarkable the fact that even though layer charge is recognized as one, if not the most determinative property of the smectitic family to comprehend its general interaction behaviour, there is a lot to be studied about its distribution in any bentonite occurrence, the influence of digenetic processes and alteration on this distribution and about proper methods for estimation.

On the other hand, the bentonite deposit in Melo, North Uruguay, has been described as a almost monomineralic clay consisting of dioctahedral Ca smectite formed from alteration of rhyolitic volcanic ashes, which were deposited in lagoonal to transitional environment belonging stratigraphycally to Late Permian. This implies that it may constitute one of the oldest exploited bentonite deposit known and yet it's been kept under remarkably well preserved conditions without any signs of illitization. This rare characteristic is perhaps specially related to the geological context linked to an intracratonic basin (Paraná Basin). Therefore it represents an outstanding source for academic research to gain additional knowledge about the digenetic process itself and also the way physical and chemical properties can be spatially distributed.

To achieve a complete perspective of the implications that a rational layer charge variation could have upon industrial uses of bentonites, the present research project also evaluates organophilization over a set of samples selected by layer charge variance criteria. These results will provide enough information about the actual layer charge spatial variations on the sorption properties of montmorillonite.

The present project has been developed as a Joint research between the Technical University of Crete and Universidade Federal de Rio Grade do Sul, under the supervision of George Christidis (TUC) and Prof Norberto Dani (UFRGS), As a master thesis to for the Erasmus Mundus Program "International Master in Advanced Clay Science" and with the financial support of the Clay Mineral Society (CMS)

1.2 - Abstract

The Choiyoi igneous province from San Rafael block located in central Western Argentina (Patagonia) should be considered as source for rhyolitic ash fall deposits during the earlier to mid Permian at the south section of the Parana Basin, in this context, the bentonite bed at Bañado de Medina, located 20 Km from Melo, Northern Uruguay is an outstandingly well preserved stratiform bed considering the age of deposition. It may constitute one of the oldest known bentonite deposit without signs of illitization and having economic potential. It derived from an early alteration in a lagoon to transitional environment, and it was protected from diagenesis due to the special geological situation linked to a intracratonic basin, presenting evidence of burial with a compact appearance but low diagenetic conditions, more locally it was probably conserved from erosion due to a series of faults also evident in field.

To model the spatial distribution of key smectite properties, four profiles were sampled, two coming from boreholes and 2 from fresh cut samples over the mining front, Forming roughly an Isosceles Trapezoid with a median of approximately 100 m; 21 samples were analyzed over the four profiles. Bentonite bed ranges in the studied area from 5 to 6 m thick underlying top soil layer and overlaying a gross grain sandstone layer. Mineralogical composition observed on whole rock XRD traces showed an increasing content of the smectitic phase as a function of depth, going from 30% to 50% at around 1,5 m depth to 90 to 96 % at a depth ranging 7 to 8,3 m depth, varying very slightly from one profile to another but keeping the trend. Mayor mineral phases identified were Mg rich dioctahedral montmorillonite with mainly Ca in exchangeable position, Quartz, feldspar (Albite and K-feldspar) and only occasionally as trace phases we observed Illite and Zeolites (heulandite-clinoptilolite). XRF chemical analysis results are also coherent with this vertical tendencies, expressed in a notable decrease of a SiO_2, K_2O, Na_2O indicating less quartz and feldspar species; and with increasing of MgO as octahedral substitution representing the main source of layer charge, Al_2O_3 most octahedral but also in a rather small amount as tetrahedral substitutions, Fe_2O_3 presumably octahedral and CaO compensating electrical charge desequilibrium.

Layer charge was estimated on the <1 μm size fraction by two methods and spatial distribution shows a clear trend to increase at the middle of the bed up to values around 0,56 e/huc and decrease towards top and bottom over values ranging from 0.46 to 0,48 e/huc. This gradual variations can be better observed on the XRD patters than by actual layer charge calculation methods results, given the fact that for this slight variances, commonly used methods are not sensible enough, Nevertheless the 001 peak position and shape of the smectite phase represents sufficient evidence for conclusions. Layer charge distribution is mainly Octahedral derived from unit formula calculations and Layer charge is clearly heterogeneous due to Organophilic sorption and swelling behavior observed.

Cation exchange capacity was calculated by ammonium acetate method, values obtained are directly proportional to layer charge estimations over those samples. CEC values around 110 moles/100gr of clay correspond to Layer charge on the order of 0,55 e/huc and values around 90 moles/100gr of clay to layer charges around 0,46 e/huc. The amount of dodecylammonium Chloride ($C_{12}H_{28}ClN$) used for organophilization was established proportional to the CEC average. Regarding the implications on physical properties and organophilization, XRD patterns of Organophilic clays showed a tendency on expandability as a function of layer charge in terms of their 001 ($C_{12}H_{28}ClN$)-

Montmorillonite peak position, ranging from 17,05 Å To 17,68 Å. They could all be considered as bilayer intercalated Organoclay complexes, classically expected at 17,46 Å according size of the alkyl chain used, and the known sorption isotherm. The slight variances are indicating the presence of non-intercalated sheets due to charge heterogeneity. Despite the slight d-spacing differences among samples, the relationship 001 Organophilic C profile as a function of layer charge has a perfect correlation. Comparing a single profile, 001 d-spacing of organoclays tends to increase with increasing layer charge. The position of the 001 peak ranges between 17.15 Å and 17.5 Å and the raw 001 peak area after organophilization can vary from 2620.6(cps x deg) to 418.8 (cps x deg).

The tendencies observed for layer charge spatial distribution are probably related to gradual variations of permeability and water/rock ratio during alteration, the middle zone of the bed that concentrates higher values of layer charge also has showed very frequent presence of spherulitic textures that may belonged originally of opal-CT but replaced by recrystallized quartz unlike top and bottom of the bed, also Zeolites XRD traces were only found in samples located from 4 to 6 m depth, indicating that water rock ratio close to the threshold where Zeolites are favored with respect to smectites as a product of alteration.

CHAPTER II

Generalities

2.1 – Location

The bentonite deposit at Bañado de Medina, object of this study is located about 20 Km South West of the small city named Melo, on the road to Fraile Muerto, Northern Uruguay, as shown in the satellite image (Figure 1)

Figure 1- Geographical location of the Bentonite deposit at Bañado de Medina

There are two overlapping properties in the deposit 84 and 162 Hectares respectively, basically Cattle farms constituted by flatlands “Pampas” that are very characteristic of the region. The area exposed for mineral exploitation is just few hectares from which only a small portion has been used so far as exposed in the georeferenced map below (Fig. 2).

2.2 -How to get there

Perhaps from Porto Alegre, Capital of Rio Grande do Sul- Brazil, the best way to get there is by following the coastline road heading south, nevertheless and for logistical reasons we first stop in Caçapava do Sul, approximately 250 Km SW of Poa by the BR 290. Then we took the RS 357 road direction SW followed by BR 473 Until we reached Bage. And then on the same road we crossed the borderline Uruguay-Brazil thought Acegua to continue South on National route 8 for some 60 km towards Melo. Finally To find the Bentonite deposit at Bañado de medina one has take national route 7 on direction SW for 17 Km, turn left at the crossroad with route 26 and the main gate of the quarry will be just 2 km ahead on your left.

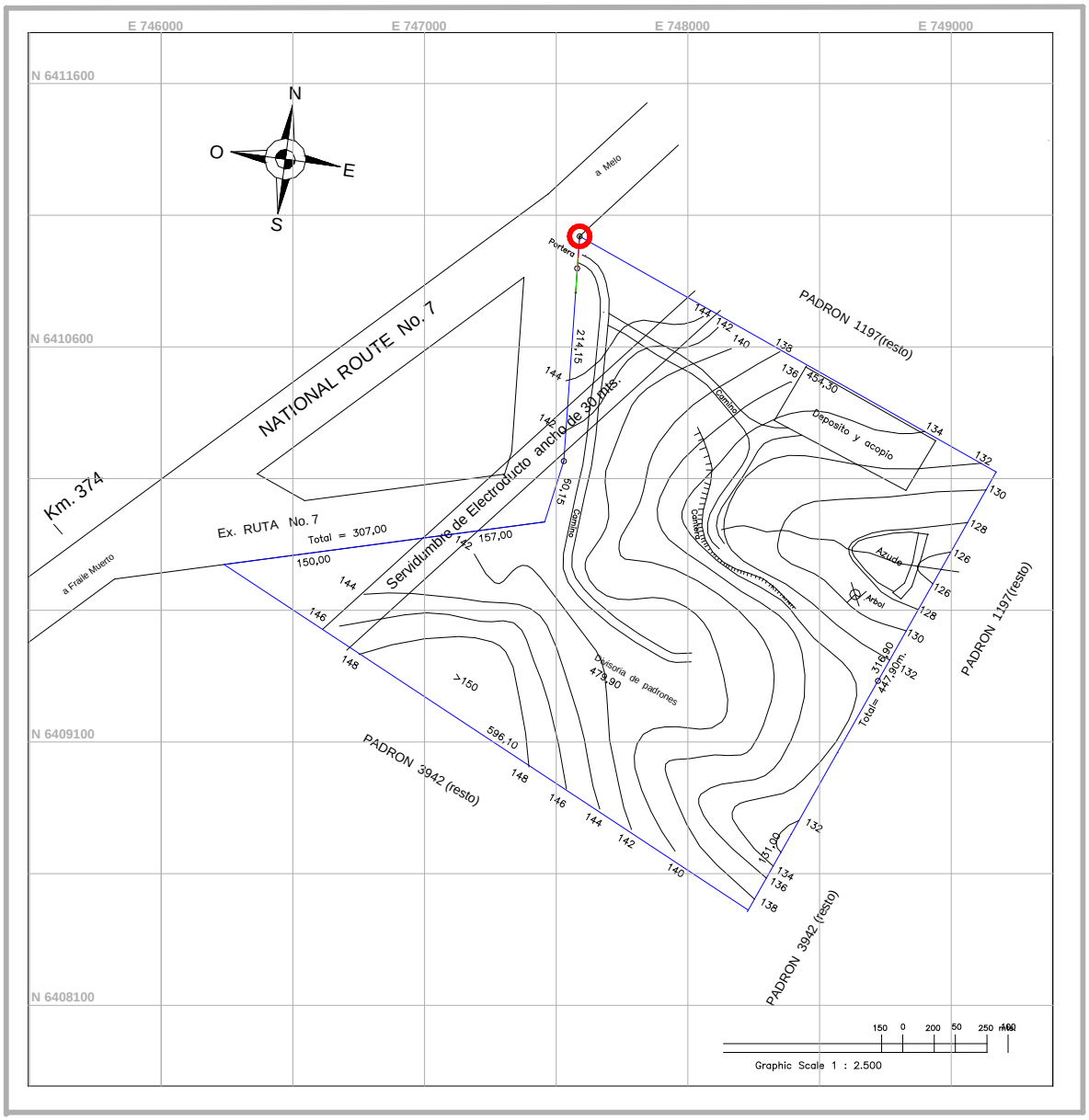

Figure 2 - Georeferenced map showing the location of the Melo bentonite deposit and detailed topography (1 m contour lines).

The blue polygon outlines the perimeter of the mining are and the deposit boundaries are shown in fig 2. The reference point is red "Portera"[1] was used to link the field geographical data obtained with a 12 channel Garmin GPS with the base map containing detailed topography acquired with total station provided by the mining company.

2.3 - Geological Context.

[1] UTM coordinates for the referenced point are given in chart 2.

The Bentonite deposit named as Bañado de Medina located 18 Km southwest from Melo, Northern Uruguay, has been characterized and geologically described as an essentially monomineralic clay containing dioctahedral smectite mainly with Ca exchangeable cations in the interlayer position (Calarge et al., 2001). It evolved from the alteration of volcanic ashes deposited in a lagoonal to transitional environment that belongs stratigraphycally to Late Permian Rio do Rastro Formation (equivalent to Yaguari Formation in Uruguay, Andreis et al., 1996, Rocha-Campos et al., 2010). This implies that it may constitute one of the oldest bentonite deposits known and yet it's been kept under remarkably well preserved, due to the special geological context linked to a intracratonic basin (Paraná Basin) and more locally due to a series of faults that protected the rather thin bed from erosion. Therefore it represents an outstanding source for academic research to achieve more knowledge about the digenetic process itself and also the way physical and chemical properties can vary as a function of their spatial distribution.

The bentonite bed at Bañado de Medina has been correlated to a regional scale of rhyolitic volcanic source occurrences, (Coutinho et al. 1981, 1991), where the volcanic source was probably located in southwestern Argentina and Chile. Formoso et al (1998) dated the bed as Earlier to Mid Permian. Calarge et al (2001) and Meunier et al (2005) correlated Bañado de medina to the bentonite occurrences at Acegua, Southern Brazil, based upon mineralogical similarities and chemical signature of heavy minerals and rare earth elements (REE). They suggested that variations in major element, RRE and minor element abundances throughout the massive clay deposit indicate two successive ash falls. Moreover, the abundance of trace elements indicates a fractionated volcanic glass derived from rhyolitic magmas produced in a subduction/collision geological context.

About the volcanic source and in a more regional scale, a precise work was presented by Rocha-Campos et al (2009). These researchers stated that the Choiyoi igneous province from San Rafael block located in central Western Argentina (Patagonia) should be considered as source for the ash fall deposits during the Permian section of the Parana Basin, along the Pacific margin of Southwest Gondwana and the geological evolution of neighboring Paleozoic Foreland basins in South America and Africa. Figure 3 shows a geographical influential spectrum of the volcanic ash source. Although Melo has been dated as Permian, it is also accepted that volcanic activity in Northern Patagonia reached an activity peak in the Triassic and early Jurassic (Andreis *et al*, . 1996) and these events have been described as more highly explosive due to the felsic nature of the magmas (Axelrod, 1985).

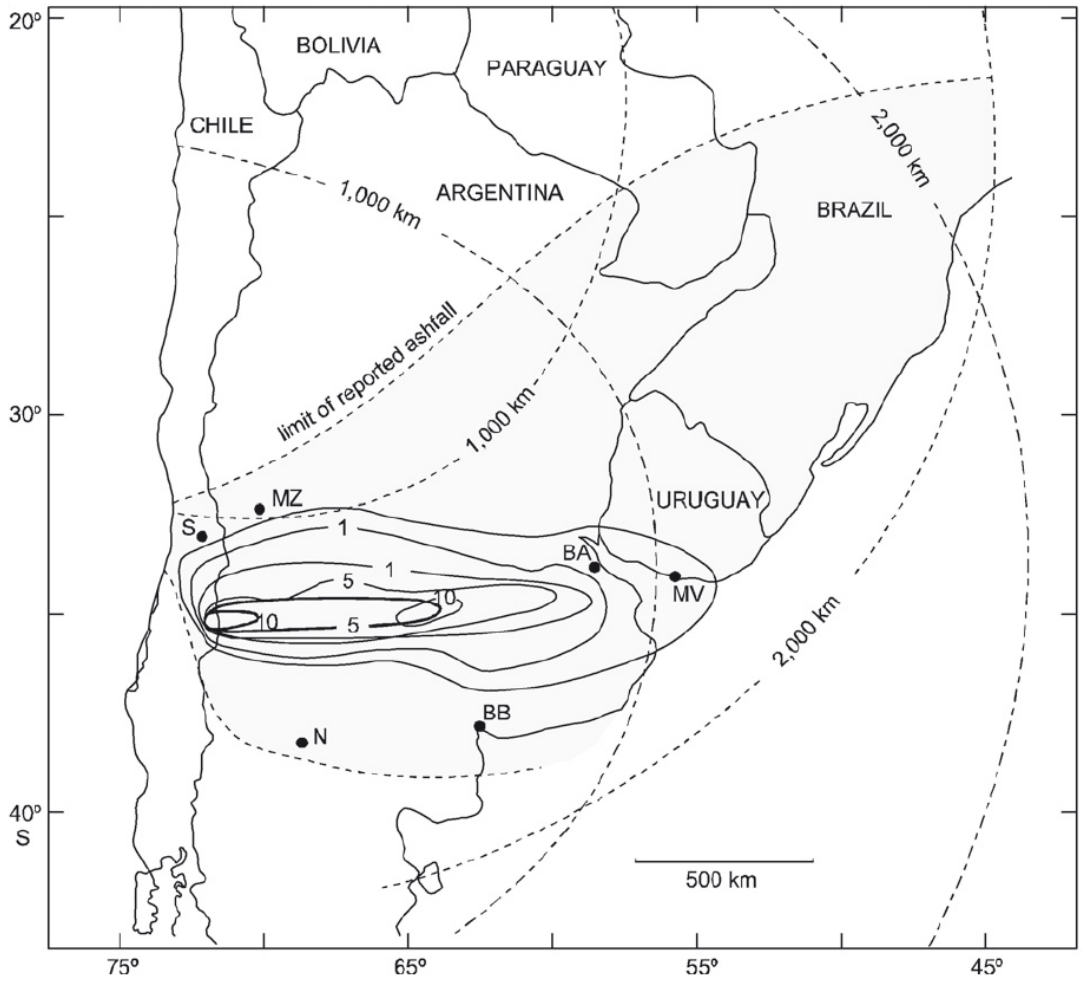

Figure 3 - Circles at 1000 and 2000 Km radius centered on the San Rafael area and Northeastern Choyoi igneous province towards the Parana Basin; Base map: ash distribution during the Quiza pu eruption of 1932 (Hiltrech and Drake, 1992). Coarser contour lines: ash fall thickness by Larsson (1937). MZ: Mendoza; BA: Buenos Aires; MV: Montevideo; S: Santiago, N: Neuque; BB: Bahia Blanca. Through less intense, the eruption exemplifies dispersion of ash over distances comparable with those of Choiyoi Volcanism. (After Rocha-Campos et al. (2009)

2.4 - Background

2.4.1 - Justification for this research

The project has been justified in the introduction regarding the importance of layer charge spatial distribution and possible implications on industrial applications of bentonites, nevertheless there are other aspect of this investigation that are worthy to be mentioned:

1. At the moment the small quarry in Bañado de Medina is being mined with opencast methods without mixing criteria or homogenizing throughout the different fronts. About 25% to 35 % of the 9 m to 7 m typical profile is discarded; only the very high smectitic section of the bed is currently exploited. XRD traces in the current research show how at depths 1.5 m - 2,2 m from the top soil have a significant dioctahedral montmorillonite content that can vary from 60% to 25%. Such is the case of profiles F1, C and F2 (Fig 3 - F1 profile whole rock XRD as a

function of depth), According to the end uses mixing of materials with different montmorillonite contents could be convenient in order to extend reserves and service life for this deposit.

2. At a regional scale, the implications of the results derived from this research could provide valuable prospection criteria, considering that the volcanic source for this bentonite deposit was located in the Argentinean Northern Patagonia and was active until the Late Jurassic. The distance from the source to the deposit constitutes sufficient reason to believe that is very possible to find similar deposits of economical interest in the broader area. Similar beds, though with insignificant thickness, have been found in South Brazil. By understanding the diagenetic conditions of this deposit and all preserving variables one could establish parameters to predict other possible occurrences. At a more global scale, this deposit represents a unique opportunity to study a bentonite deposit with the characteristics mentioned before, and this is perhaps the first attempt to do so under this perspective. In addition, by going deeper into how the layer charge of this deposit varies and how it affects all physical properties, we could draw conclusions that will enable to predict qualities of other deposits as a consequence of their own diagenetic process.

3. The fact that estimation of layer charge will be performed by two different methods[2], will provide a good comparison over a set of samples with different layer charge values and just above the error margin of the methods.

2.4.2 Related studies about Melo.

The bentonite occurrence has been first reported by Goñi (1952) an then by Bossi (1966). In the section “Geological context” (page 6) there is a complete description of the whole evolution regarding the geological origin of Melo Bentonite deposit and a chronology of related research. However, there are other investigations that were consulted along the progress of this work that they also provided valuable information.

The research performed by Calarge et al (2003) proposes the idea of layer charge heterogeneity for this deposit as a function of swelling capability. Although these authors describe the stratiform bentonite as a 1,5 m thick smectite rich bed, which contains less than 5% non clay minerals. In contrast the current research showed that the highly pure bentonite bed can be up to 5 m thick and its mineralogical composition vary widely

[2] Christidis Eberl method (Christidis E. G. et al,. 2003), Uses XRD traces and swelling behaviour after K-saturation and Ethylene glycol solvation, and Classic structural formula method feeds from XRF chemical analysis over the ,1µm size fraccion size.

particularly at the top. On behalf that publication one can say that the exposure of a whole perspective at the quarry is a rather recent event. Calarge et al.(2003) proposed a layer charge of -0,45 per half unit cell[3], and the presence of smectites randomly interstratified in terms of layer charge magnitudes, to explain layer charge heterogeneities and the observed presence of non-expandable layers. This idea seems to be in agreement with what was observed in this work in the spatial distribution of layer charge and we will comment further on this later on at results.

Several works developed at UFRGS about Bañado de Medina where also consulted. Published work on the geology, mineralogy and technological applicaitons of Melo bentonite by Delfino et al. (2009) Under the name of "Jazida de Bentonita de Banado de Medina,Melo,Uruguai. Geologia, Mineralogia e utilizacao tecnologica". presents a very detailed geo-structural model derived from a series of 31 Boreholes. This campaign provided samples of profiles B and C used in the present investigation. The CEC of the bentonite varied between Between 101 and 116 meq/100g and the bentonite reserves were estimated to be 580.000 metric tones.

2.4.2 Related studies on Layer charge

The Clay Mineral Society (CMS) published on 1994 the workshop lecture, Volume 6 named Layer charge characteristics of 2:1 silicate clay minerals. It is a key document used as a ground base to interpret interactions between montmorillonite and amines as a function of layer charge (Lagaly, 1994, Laird, 1994). Particularly the chapters developed by G. Lagaly, "layer charge determination by alkylammonium Ions", the one by D.A. Laird "Evaluation of structural formula and Alkilammonium methods of determining layer charge". And Specially the one offered by S.A. Boyd and W.F. Jaynes. This work was also used as a reference of related studies about organophilization.

Christidis & Eberl (2003) proposed one of the methods used in this research to estimate layer charge and charge heterogeneity. The mentioned publication explains how from 29 well characterized samples loaded on a data base, is possible to compare XRD patterns after potassium saturation and ethylene glycol solvation to obtain layer charge magnitude and heterogeneity from profile fitting or by peak position criteria. The layer charge program that resulted from this work was written on Visual Basic and the code employed

[3] This value is among the range of layer charge magnitudes obtained in this study, tending towards the lower limit. (from -0,44 to -0,56 per half unit cell)

by macro function of Microsoft Excel. This software was provided by George Christidis, co-supervisor of the present research to the author.

The journal “Elements”, Vol 5, April 2009, published an issue devoted on bentonites. Christidis & Huff addressed the topic of layer charge and provided a broad overview about the variables which control bentonite formation and alteration. This publication showed evidence for cryptic variations in bentonite deposits, as was reported by Christidis and Makri (2007) in a bentonite deposit located in Milos-Greece and in a 1 m thick bed in Charentes, France by Alain Meunier et al (2004).

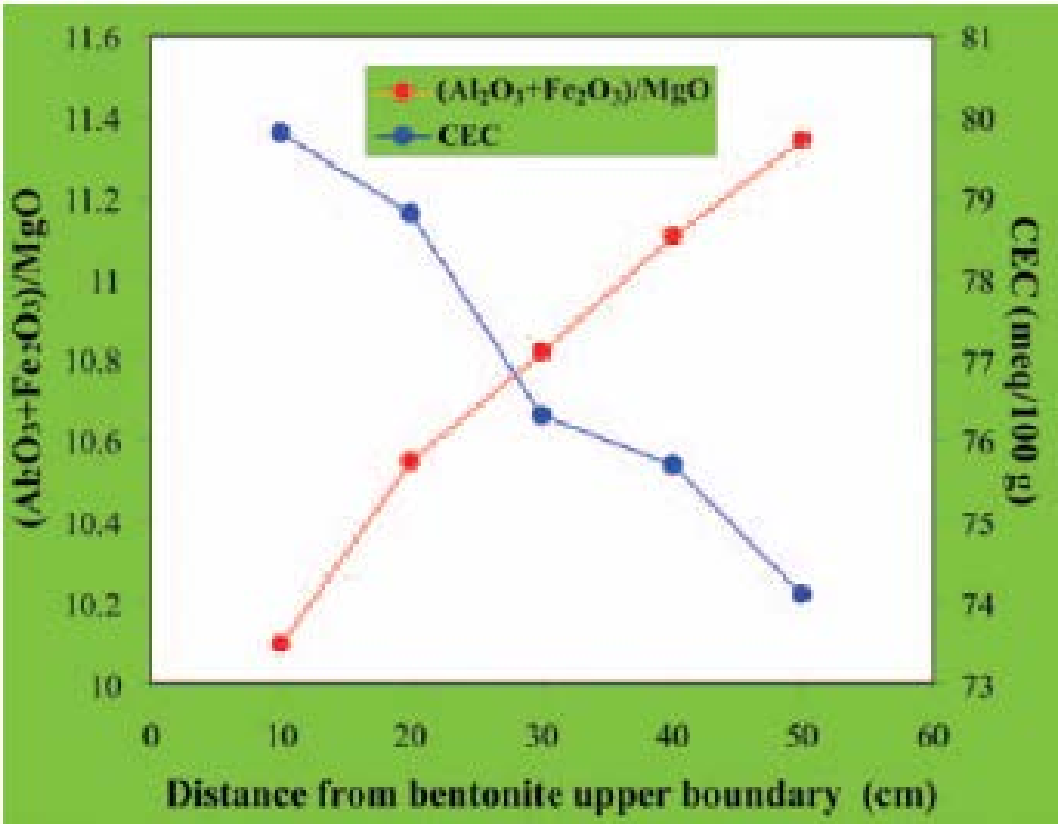

Figure 4 – Variation of C.E.C and the $(Al_2O_3+Fe_2O_3)/MgO$ ratio with depth in Smectites from a Bentonite deposit located in Charentes, France. Data from Meunier et al (2004) (after Christidis & Huff, 2009)

2.4.3 - Related studies on Organophilization

It is widely accepted that layer charge is the most important parameter of smectites when organophilization is intended (A.R. Murray, 1994). Nevertheless, It is classically C.E.C the parameter used to estimate the amount of amines that will be added in the process. Although C.E.C and layer charge usually should be directly related, there are other parameters that may affect this relationship, such as crystal size, stacking sequence and arrangement, charge density, etc. Nevertheless this topic is not a matter of this research.

On the other hand, industrially it is perhaps the proportion of the smectite present in a given bentonite the main factor to take into account, not only for organoclays but also in any kind of activation and many other processes.
Therefore, is important to outline that organophilicity itself if is not the purpose of this research but a mean to evaluate a tangible influence of layer charge spatial variations on the efficiency of the amine-clay intercalation.
Basic evaluation parameters and principles where extracted from The Clay Mineral Society 1994 workshop lecture, Volume 6, chapter by S.A. Boyd and W.F. Jaynes "Role of Layer charge in organic contaminants sorption".

Other Important readings were.

- Clay sorbents: the mineralogy, processing and applications by Murray (2005).
- Sorption and Detoxification of Toxic Compounds by Bifunctional Organoclay, by Gerstl et al. (2004).
- Adsorption of polyamine on clay minerals by Blachier et al. (2009).
- Uses of Organo Clays by L. Deligianni, A. Ekonomakou, Bentonite Division- Silver & Barite Group. (2010).

CHAPTER III
Methods and material

3.1 - XRD

All 21 samples were analyzed on XRD as non oriented powder and less that 1 micron size fraction to acquire almost monophase diffraction pattern. Whole rock analysis will establish mayor mineral phases present; homogeneity of trioctaheral nature for Montmorillonite and together with SRF chemical analyses through molar estimations is also possible to establish a semi-quantitave comparison of mineral phase's proportions, present in each pattern, and how it fluctuates as function of depth. As for the clay fraction size, Air dried samples vs. ethylene glycol solvated will determine swelling behaviour. Also Sodium saturation[4], Potassium saturation and Organo-clays where analyzed, Finally XRD patterns from a potassium saturated and ethylene glycol solvated will be compared to a XRD simulated traces calculated from three component interlayering as established in the Christidis Eberl method (Christidis E. G. et al,. 2003) for layer charge estimations. All specific preparation procedure is explained later on in this text. Parameters and equipments used are specified on the following table.

Sample preparation	Number of Samples	2 Theta range	Step Size	Time per Step	Diffractometer and radiation source
R.O.P.	21	From 4° to 75°	0,02	3	Siemens - Bruker-AXS D5000 CuKσ radiation (40 Kv , 30 mA). Graphite monocromator
R. O. P. (F1 profile only)	3	From 4° to 75°	0,02	2	D8 Advance of Bruker with lynxEye multi-channel detector. CuKσ radiation (40 Kv , 30 mA).
Air Dried O.S,	21	From 2° to 35°	0,02	3	Siemens - Bruker-AXS D5000 CuKσ radiation (40 Kv , 30 mA) Graphite monocromator
EG O.S.	21	From 2° to 35°	0,02	3	Siemens - Bruker-AXS D5000 CuKσ radiation (40 Kv , 30 mA) Graphite monocromator
Na- Saturation O.S.	9	From 2° to 20°	0,02	2	D8 Advance of Bruker with lynxEye multi-channel detector. CuKσ radiation (40 Kv , 30 mA).
K Saturated+ EG O.S.	21	From 2° to 35°	0,02	2	Siemens D500 XRD, CuKσ radiation (40 Kv , 30 mA) Graphite monocromator
Organophilic Montmorillonite O.S.	12	From 2° to 20°	0,02	2	D8 Advance of Bruker with lynxEye multi-channel detector. CuKσ radiation (40 Kv , 30 mA).

Table 1- Parameters and equipment used on X-ray diffraction.
All oriented slides where done over the less than 1 μm particle size.

- R.O.P. = randomly oriented Powder
- O.S. = Oriented slide
- EG = Ethylene Glycol solvated

Sample Preparation:

[4] Only a pre-step for Organophilization to create a greater gap between the 001 Montmorillonite peak before and after amine intercalation to distinguish better the efficiency of amine absorbed onto the interlayer space. It will be analyse only selectively as a function of layer charge just as a way to track the Na saturation process.

Whole samples where gently ground with pestle and mortar. Ten representative samples were selected with spatial position criteria; subsequently they were wet sieved to obtain >53 μm fraction for observation of heavy minerals. Afterwards the > 1 μm size fraction was obtained by sedimentation according to Stokes law using deionised water. Ethylene Glycol treatment was done in rounds of no more than 5 samples at a time to avoid evaporation of ethylene glycol; samples were put in a glass desiccator at 60°C for a period ranging 16 hrs to 24 hrs.
Na and K saturation was performed on the <1 μm fractions using 1M NaCl and KCl solutions respectively. The samples were saturated for at least 4 times, the last one overnight under mechanical agitation. Each time the solution was changed. After saturation the samples were rinsed shortly by dispersing the clay fractions with an ultrasound device and finally washed four times with ethyl alcohol.

3.2 SEM

Scanning electron microscopy was performed in a JEOL 6060 SEM. The samples were mounted on metallic stubs using a double stick electrically-conductive carbon tape,and coated with gold and carbon as is usually done in UFRGS geosciences department for better imaging. Only morphology was observed because there was no EDX analysis available.

3.3 Optical Microscopy.

The optical microscopy was performed with a Leika DMLP optical microscope. Freshly cut bentonite samples were mounted on petrographic slides with a special glue to avoid fracture when swelling. Then they were dry polished to ~ 100 μm thickness.

3.4 TG analysis

A set of 20 samples were analyzed on a PerkinElmer thermo-gravimetric analyzer TGA 6. The thermal analysis was run up to 920° C on a heating ramp of 20 C° per minute. Samples where finely ground and the initial mass used varied from 15 mg to 30 mg.

3.5 XRF analysis

Chemical analysis of whole rock and <1μm size fraction was determined using the X-Ray fluorescence (XRF) technique, using an S 2 Ranger EDX spectrometer by Bruker. A total of 42 samples[5] and ten random control duplicates were used to prepare fusion beads. Loss on Ignition (LOI) was determined before melting following the procedure explained

[5] 21 Whole rock samples and 21 <1 μm samples

in next paragraph. Fired powders after determination of LOI were mixed with Lithium tetraborate ($B_4Li_2O_7$) flux under the following conditions:

1. Mixing proportion whole rock:flux was 5:1[6].
2. Mixing proportions for most <1 μm fractions was 8:1[7]. Although some samples had a different proportion this ratio was kept and used in the instrument software settings to calibrate concentrations.
3. Samples were gently ground, and weighed, then $B_4Li_2O_7$ was added progressively to obtain a homogenous powder, subsequently the mixtures were placed in platinum crucibles and finally three drops of lithium bromide (BrLi) were added and the samples were melted in a Claisse M4 gas Fluxer to obtain the fusion beads.

3.6 Loss on Ignition (L.O.I.)

L.O.I was estimated for all 42 samples and 10 aleatory selected duplicates by following this steps:

1. Porcelain crucibles were weighed after drying in an oven at 110ºC.
2. Each crucible was labeled and filled with a powder either of whole rock or <1μm particle size, dried for at least 3 hrs at 105ºC and weighed. Then the dry weight of the samples was recorded.
3. Subsequently the powders were fired for 2 hrs at 1000ºC. Finally from the difference of the weight after drying and and after firing, the LOI was estimated.

3.7 Cation Exchange Capacity (C.E.C) estimation.

C.E.C was estimated by the Ammonium Acetate method (NH3) and concentrations were measured using a Spectrometer with Lithium-Ion Battery Hach DR 2800. A total of thirteen samples were collected selectively according to layer charge criteria, This were the same samples that later on were use for Organophilization and the intention behind CEC determination was to estimate the quantity of amine necessary for effective Organophilization, Hence the clay-organic interaction was used to evaluate the effectiveness of the process and to corroborate the trend observed for the layer charge distribution as a function of depth, provided that the two parameters should be directly correlated.

[6] 7,5 gr of $B_4Li_2O_7$ over 1,5 gr of sample after L.O.I.

[7] 8 gr of $B_4Li_2O_7$ mixed with 1 gr of sample after L.O.I.

1. About 0.5 g of the <1µm fractions was dried for 3 hrs at 105ºC and placed in centrifuge tubes; about 0.3g of dry sample was used to determine CEC.
2. 10 ml of 1M ammonium acetate were added in the tubes and the clay suspensions were agitated for 1 hour. Afterwards the solution was decanted. A second saturation with 1M ammonium acetate took place under continuous agitation for 24 hours.
3. Then the samples were rinsed four times with ethanol (30 ml each time), to remove excess acetate.
4. Subsequently the samples were leached with 25 ml of potassium chloride 1M three times. The the supernatant solutions were stored and the volume was made up to 100 ml.
5. The ammonium concentration in the solution was measured in the spectrophotometer following this steps
    a. The solutions were diluted to 5% to be in the absorbance range of the equipment[8].
    b. Then 3 drops of Mineral Stabilizer, 3 drops of Polyvinyl Alcohol Dispensing Agent and 1 ml of Nessler Reagent were added and the solutions were allowed the reaction to occur for 1 minute.
    c. The Polyvinyl Alcohol Dispersing Agent aids formation of yellow color after reaction of Nessler Reagent with ammonium ions. The color intensity is proportional to the ammonium concentration. The absorbance values obtained were then transformed into ammonium concentration according to the curve shown in Figure 6

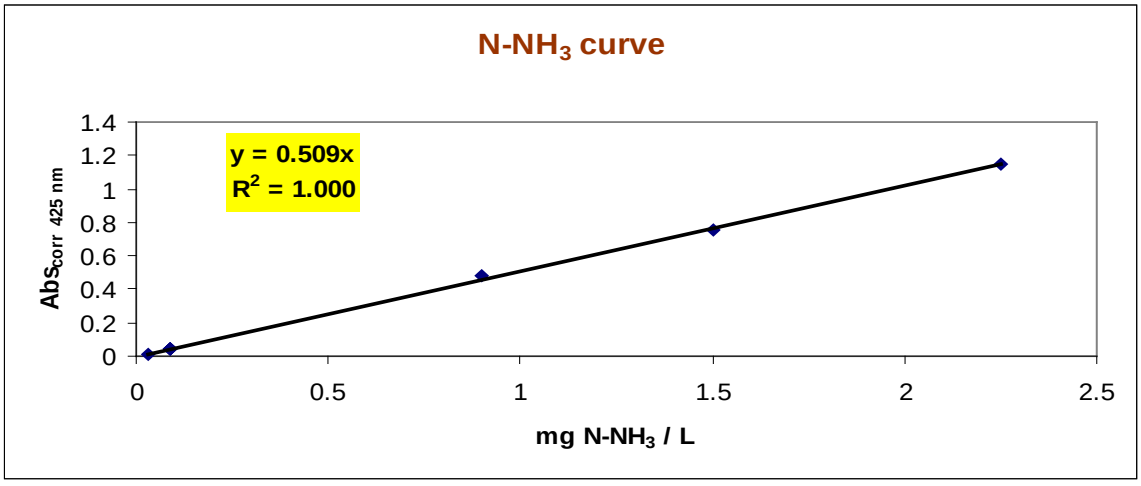

Figure 5 - Calibration curve used for determination of NH_4.

[8] • Concentration Range: 0,02 to 2,50 mg/L N-NH3

After concentration is known then we proceeded establish the relationship between this value and CEC as it is shown at table 6 located in the section of this documents that refers to Organophilization.

3.8 Layer charge determination.

Being the main object of this study to establish precisely if the layer charge is systematically distributed in the bentonite bed, the estimation of the layer charge was carried out by two methods. One of them inlvolved observing XRD patterns after potassium saturation and ethylene glycol solvation of the clay samples and subsequent comparison with XRD simulated traces calculated from three component interlayering (Christidis & Eberl, 2003). The profile fitting is done with a excel sheet that was an output of this investigation and offers at the same time two different ways to compare the measured XRD values to the data base of the LayerCharge program (Christidis & Eberl, 2003). (1)-Whole profile fitting (2) - peak position fitting. Both values were calculated and are discussed in the results chapter.

Figures 6 and 7 show a screen displayed of the two methods provided by the program of layer charge determinations described before

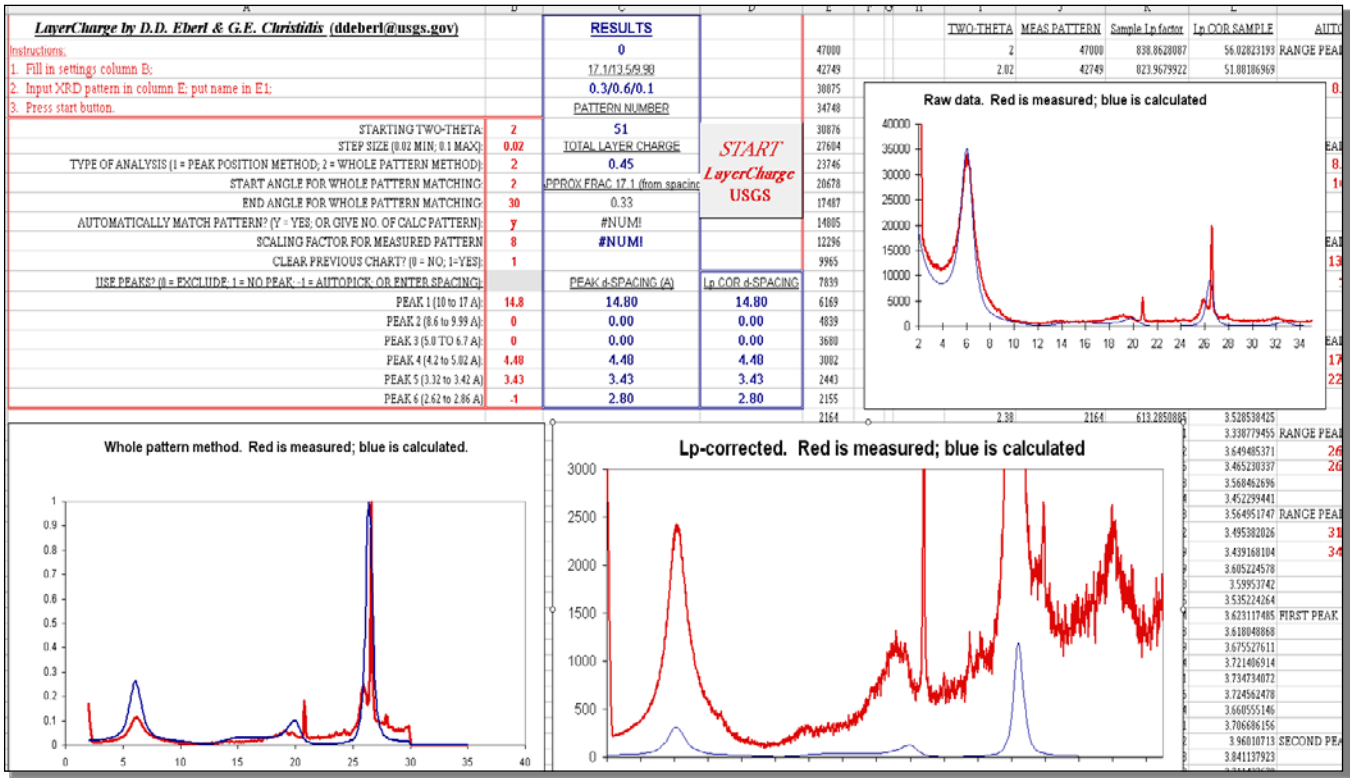

Figure 6 – Layer charge determination by Whole pattern method.

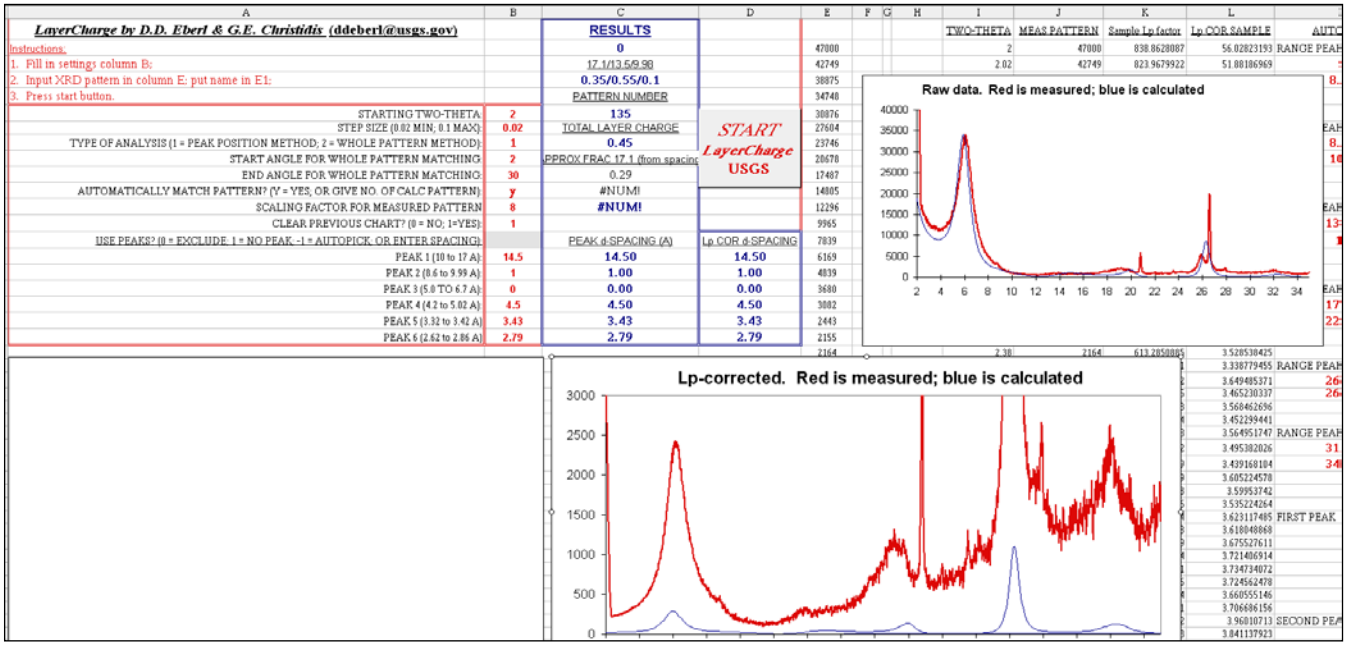

Figure 7 - Layer charge determination by peak position method

The second method uses the structural formula calculation (Schultz, 1969; Newman Eberl *et al.*,1986; Newman and Brown 1987; Onal, 2006) from the data obtained by XRF chemical analysis results in < 1 µm samples. This last method will also provide enough information about the octahedral and tetrahedral distribution of the layer charge.

A slight correction was perform to SiO_2 values of chemical data to establish a reliable structural formula for montmorillonite. In the XRD traces it is possible to notice the presence of quartz, which has a tendency to decrease as a function of depth. A semi quantitative determination of quartz was made from the 101 reflection, which was subsequently subtracted from the SiO_2 determined by XRF. The figure 8 shows an example of the C profile, were the XRD pattern of K saturated, EG solvated <1 µm oriented slides at 1.4 m depth contains ca 10% of Quartz, and the one at 8.3 m is just above the detection limit for quartz[9], 1%.

[9] For this equipment is around 0.2 to 0.3 %.

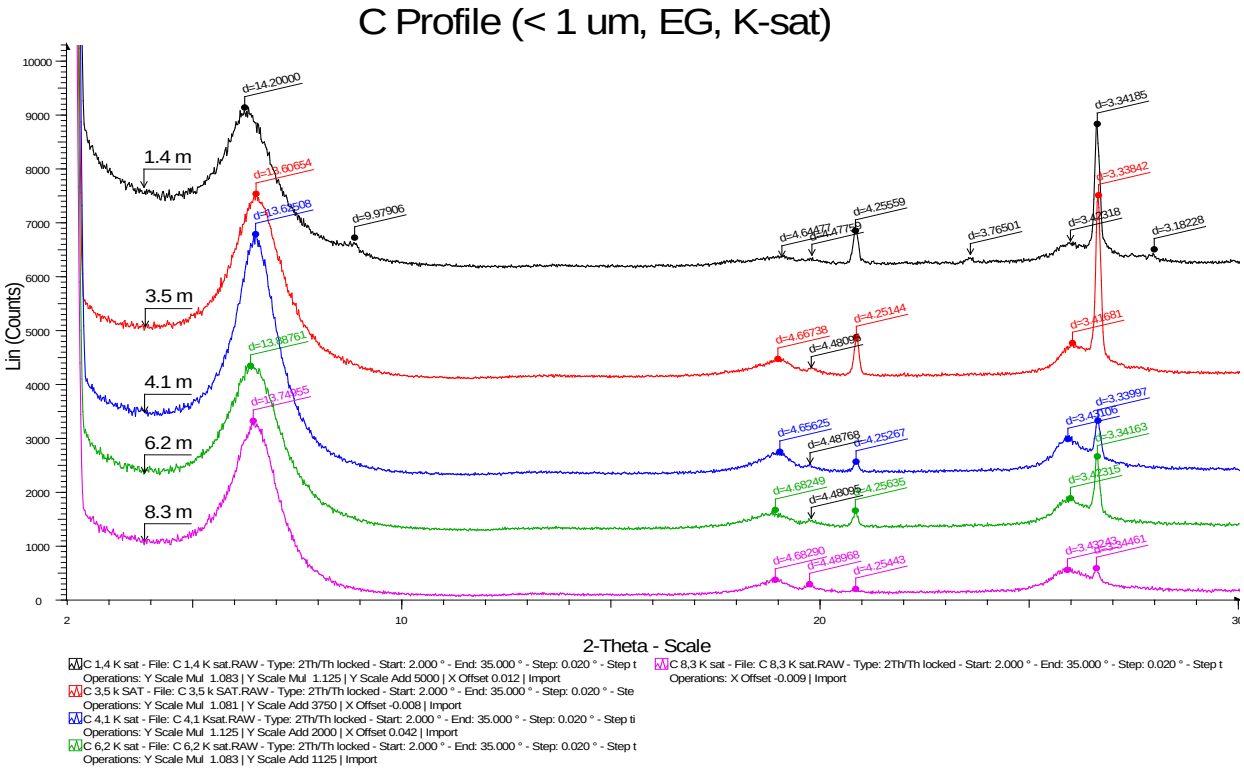

Figure 8 – XRD patters of C profile samples K-saturated and ethylene glycol solvated as a function of depth.

Note: Conclusions about Layer charge heterogeneity will derive from Christidis & Eberl method and layer charge octahedral or tetrahedral location from structural formula method.

3.9 Organophilization

The purpose of preparing organo-clay complexes in this study was to evaluate the influence of layer charge variance in Melo bentonite deposit on the capability to interact in one of most significant industrial applications of these materials. Most variables were fixed like: type, concentration of dodecylammonium chloride ($C_{12}H_{28}ClN$) and preparation of amine, ageing time, montmorillonite size fraction and amount, etc. Moreover, conditions on which organophilization was performed for all samples can be considered equal.

We used 12 samples selected according to layer charge criteria. The whole C profile was treated as a model for possible trends observed, and also samples F2 M1, F2 M2, F2 M5, F2 M7, F2 M8 and F2 M9. Profile F2 had a similar overall trend but some deviations in layer charge values as a function of depth was the reason why it was selected. Only the <1µm powder was used and the procedure followed is described below, per samples and they where prepare with the following:

1. About 0,5 g of the <1µm samples were saturated three times with Na using 30 ml of NaCl. After last saturation the samples were left overnight under mechanical agitation.

2. After washing the samples with deionized water four times, they were dispersed in dodecylammonium chloride solution 5 times. After the last run the centrifuge tubes where covered and kept for 24 hrs at 60 °C.
3. Subsequently the samples were washed five times with methanol and oriented slides were prepared also using methanol containing the organophilic clay. Due to the volatility of methanol the samples were dried rapidly (2,5 hr) and then they were placed in a desiccator to avoid moisture adsorption caption until X-ray diffraction analysis.
4. Dodecylammonium chloride solution was prepared by dissolving 18,5 gr of the amine into a mixture of 500 ml of deionized water and 100 ml of ethanol. Keeping a record of the pH change, 47.1 ml of 2M HCl was added to the solution up to a pH value of ca 7.3. and then 27,5 ml of 0.1 M HCl were used to avoid exceeding neutral pH. After 5 min of stable pH measurements the solution was completed with deionized water up to 1L and was stored for the organophilization experiments.

3.9.1 -The sorption of organic compounds

The sorption of organic compounds was evaluated by XRD after organophilization using the principles described by Boyd and Jaynes (1994) about the role of layer charge in organic contaminant sorption by organoclays Also TGA will provide another evaluation parameter by comparing thermal stability and weight loss as a function of temperature before and after Montmorillonite is intercalated.

CHAPTER IV
Results

4.1 - Planning

The figure 9 shows the original program as it was structured is order to achieve the goals described before. However, during the progress of the research it was necessary to make some adjustment, particularly due to malfunctioning on some of the analytical equipment in both laboratories involved. However roughly it represents pretty well the sequence of steps that where followed.

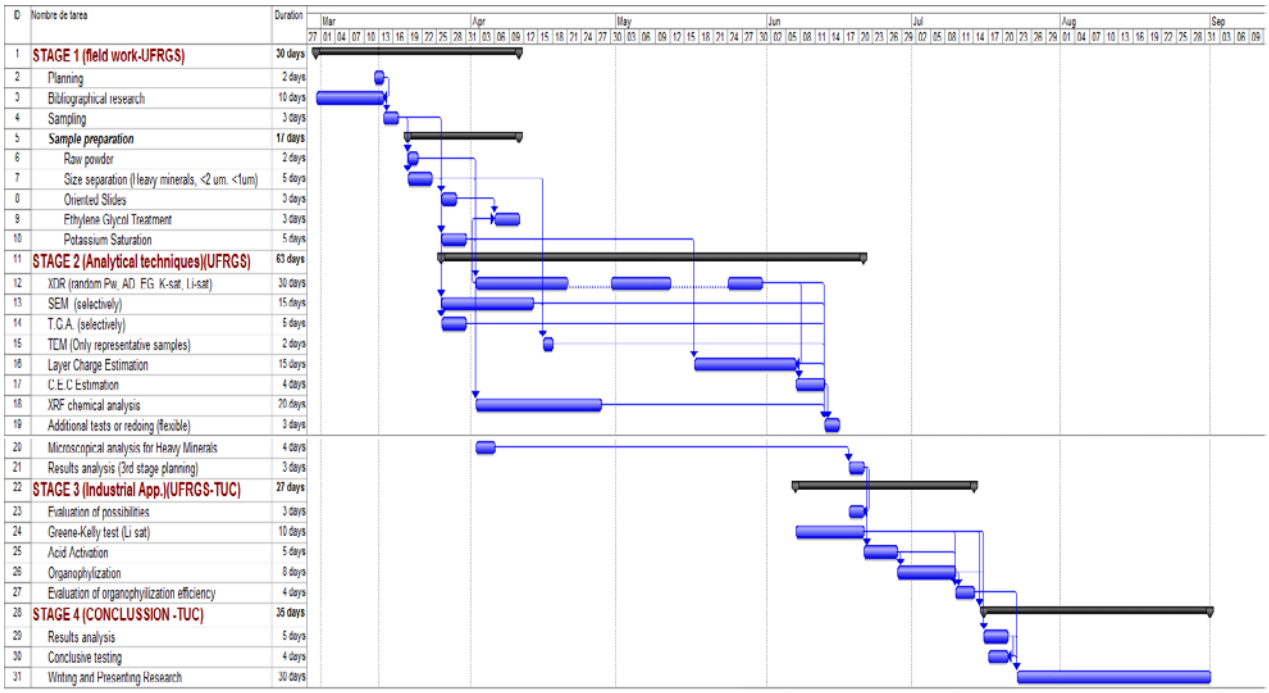

Figure 9 - Initial Research Project Chronogram

Some adjustments that worthwhile mentioning:

a) XRF was not done in Brazil, therefore results for chemical analysis were delivered in Mid August.

b) Greene-Kelly test was not performed due to time limitations, consequently any conclusions about the Tetrahedral or Octahedral nature of layer charge will be based upon results of XRF chemical analysis for the less than 1 micron size fractions of the samples.

c) Layer charge estimation from oriented slides potassium saturated and Ethylene Glycol solvated was done in Brazil for most samples. However 3 samples had to be reevaluated in Greece because the XRD patters where not totally satisfactory, since the ethylene glycol evaporated before diffraction.

d) Transmission Electron microscopy was not performed

4.2 -Field work

On March 24 a 3 days field trip to Melo began, with the following objectives:

1. Collect fresh samples from the mining fronts available.

2. Discuss with the mining company representatives in order to get access to some basic topographical data and their own perspective of the field.

3. Visit other Bentonite concurrencies on the nearby area and observe the local geological context.

4. Share Prof. Norberto Dani's ideas about the diagenetic environment and probable alteration conditions that could lead to conclusions later on in the research.

All objectives where achieved on the field work and the following Figures try to resume results. Figure 10 shows a map where all drill bores are plotted over the actual topography and in the extrapolated frame the spatial description of the 10841.35 m 2 area enclosed by the polygon created by the 4 sampled points[10].

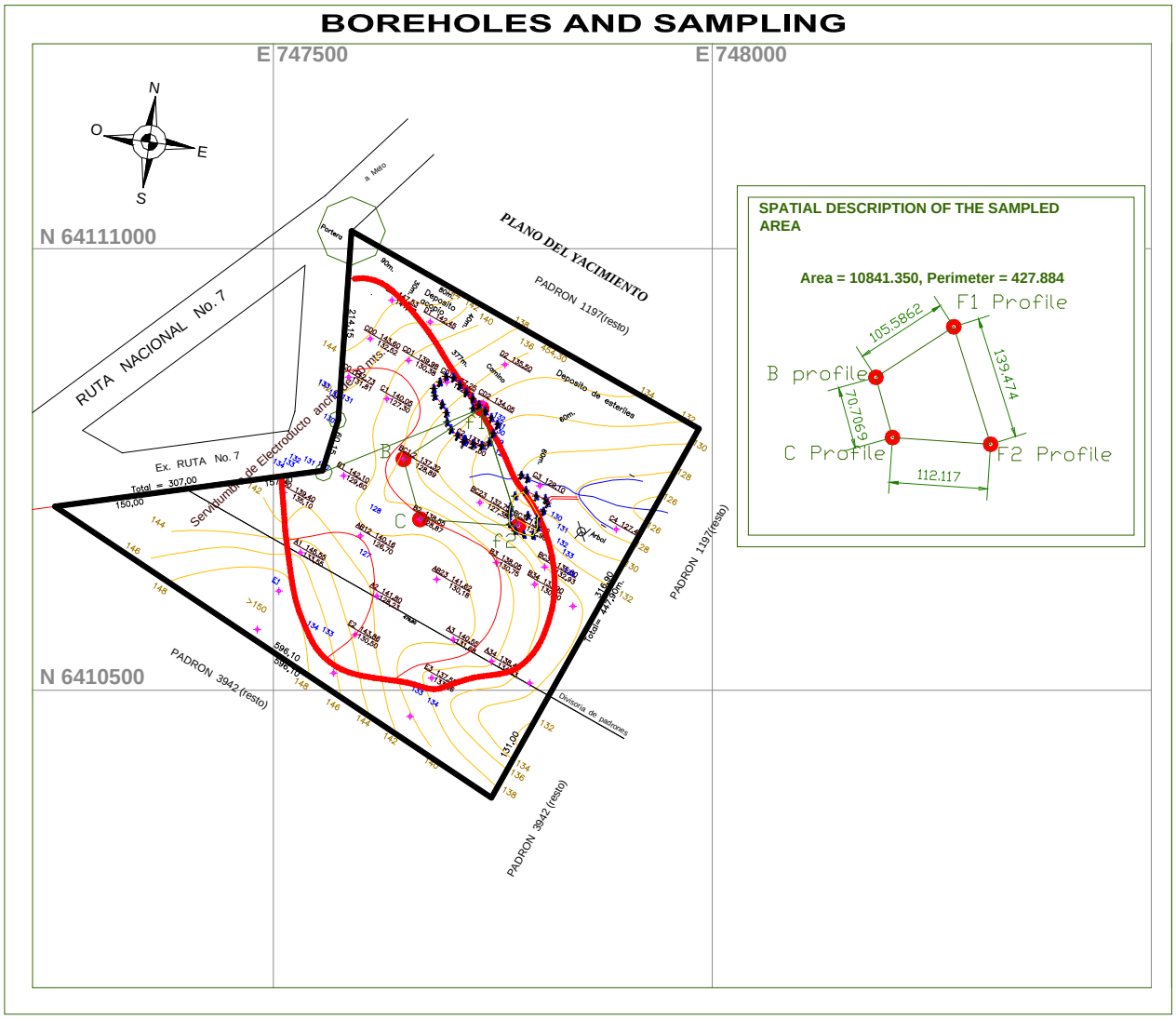

[10] Two boreholes and two fresh cut samples taken from the mining fronts, explained in detail at "Sampling criteria page 24"

Figure 10 - Location of the drill bores over the actual topography and extrapolated frame of the spatial description of the area created by the 4 sampled points.

Table 2 – UTM Coordinates for profiles location and physical reference.[11]

Point name	North	East
Profile F1	6410895	747721
Profile F2	6410686	747779
Profile B	6410761.8	747648.25
Profile C	641069.3	74766.15
Physical reference* “Portera”	6411020	747589

[11] Datum Yacare

Figure 11 - Photographs of the outcrop of Melo Bentonite (upper photo) and the F2 profile (lower photo)

4.2.1 - Sampling criteria

Four profiles were studied to establish a tridimensional view of Layer charge distribution and other relevant properties. Two of them, named F1 and F2 where fresh cut sampled on the mining front at the open cut. Profile F2 is 8.2 m high and consists of 9 samples taken by macroscopic differences and other features as shown in the figure 11. Profile F1 on the other hand only has 3 representative samples for top, middle area and bottom in order to reduce the quantity of material to be analyzed without losing the volumetric perspective of the whole study. Profiles B an C belong to boreholes taken by a research team from the UFRGS in 2009 (Delfino et al. ,2010).

Three samples of these profiles are kept in the Geological department of that University. Profile B corresponds to the original BC 1-2 and C to B2. Five samples where taken from each profile from depths that had apparent correlation, with the intention to establish a long range horizontal comparison.

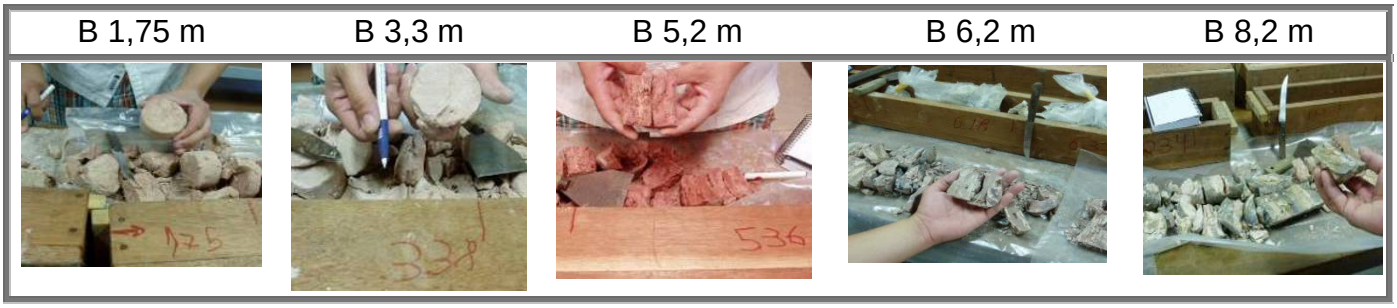

Figure 12 - Example of profile B sampling from bore holes.

It is evident that each sample has a defined and unique macroscopic appearance compared to others in the same profile. They were selected according to this divergences not with the intention to expect dramatic property changes from one to another, but to be able to correlate the horizons among the 4 profiles assuming that hence we found that they is roughly continuous log profile with depth having similar macroscopic appearance over the levels, then we are able to establish long range correlation. The main macroscopic observation are variations on the sand content, levels of high iron oxide, levels of what appears to be magnesium oxides and levels that can be called pure montmorillonitic. The following graph presents the spatial distribution of samples taken.

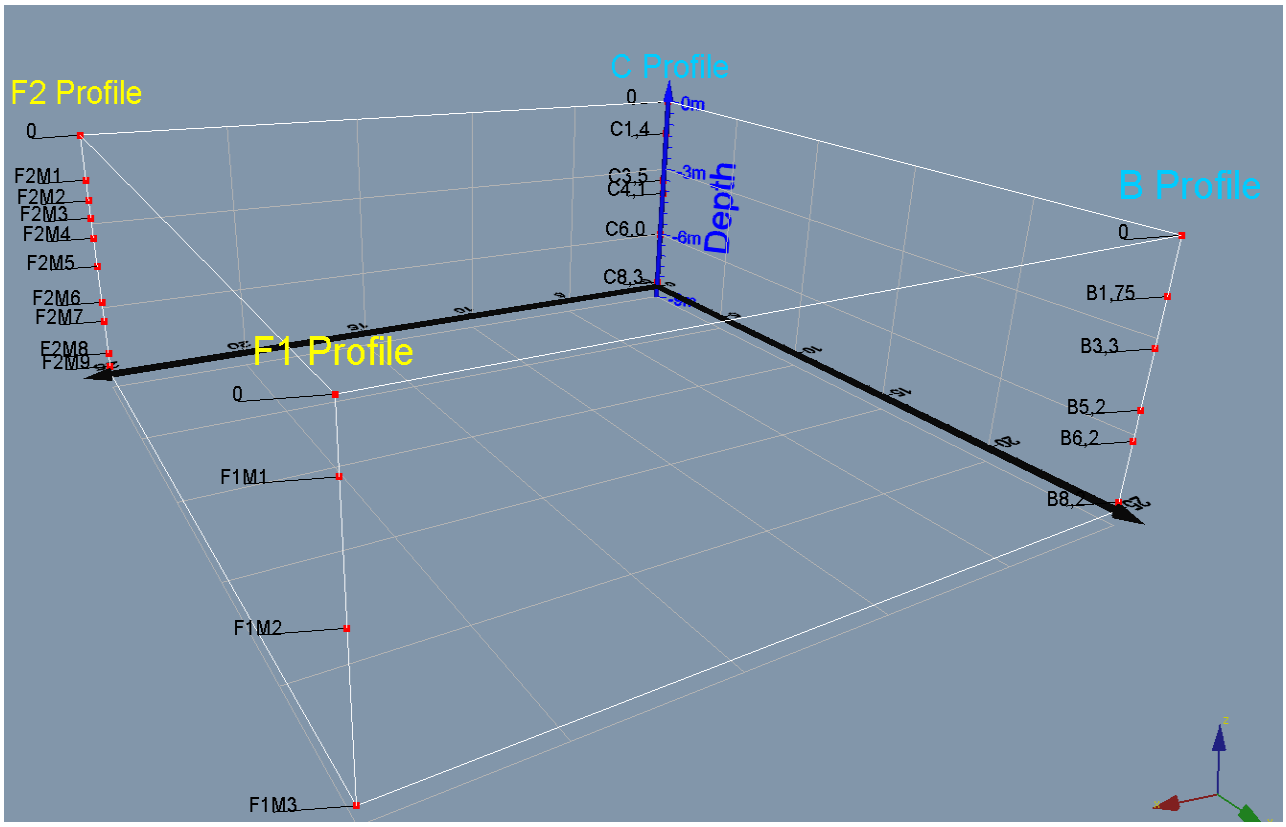

Figure 13 -Spatial distribution of samples.

Is important to outline here that some geometrical assumptions had to be impose to the 3d model in order to achieve a coherent graphical representation. These constraints are:

a) We assume that the longitudinal separation between profiles is 25 m.
b) Inner angle between any profile and the neighboring two is 90º, forming a perfect square on the surface.
c) Vertical projections and sampling depth are kept intact.
d) The slight slope shown in the topographic map is omitted.

4.3 – Mineral Phases identification and Proportions.

From whole rock XRD traces of random powder samples, it was possible to observe a variation on the mineralogical distribution as a function of depth on all profiles. Major mineral phases indentified where: dioctahedral smectite[12] and quartz, with K-feldspar and albite as minor component (Fig. 14). One of the 21 samples (profile C at 1.4 m depth) contains a small proportion of illite. Graph 14 shows the XRD trace of the randomly

[12] The reflection (060) at 1,49 A is indicative of dioctahedral smectite.

oriented whole rock sample C 6.0 m, this sample can be considered as a typical XRD pattern of the Melo bentonite throughout all profiles.

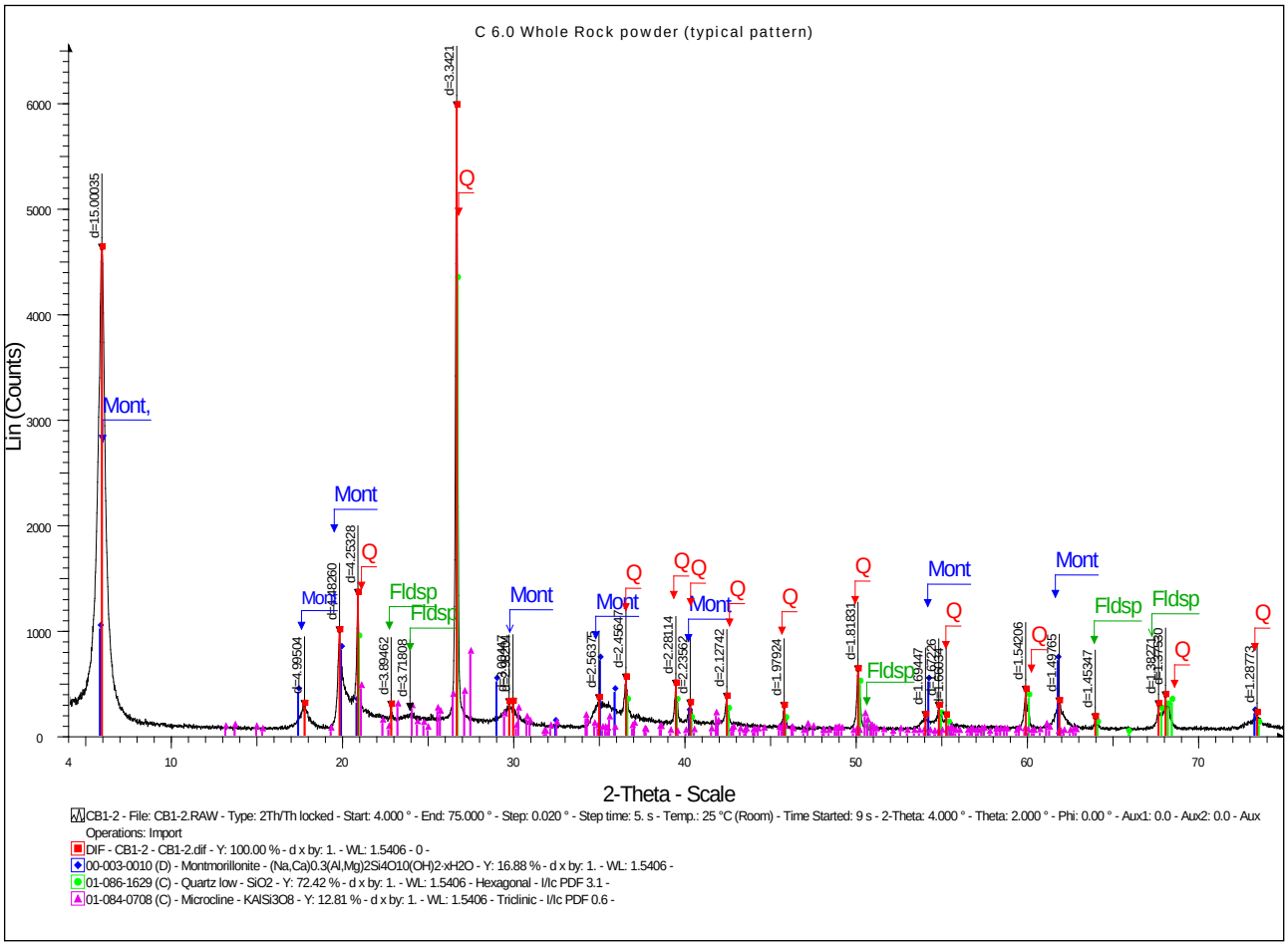

Figure 14 X-ray Diffraction pattern of random powder from sample C 6.0 (Profile C at 6 m depth). Mont: smectite, Q: Quartz, Fldsp: Felspar

Randomly oriented XRD traces for all samples belonging to the fresh cut Profile F1 are shown in Fig. 15,. In this profile is possible to observe how the proportions of smectite vs Quartz change with depth by comparing the relative intensities of the (001) smectite peak at 15 Å with the Quartz peak at 3.34 Å (101). Both phases are abundant at 2.1 m depth, then deeper the smectitic material tends to dominate over other phases up to a depth of 7.3 m were the sample can be considered essentially as monomineralic with traces of quartz and feldspar.

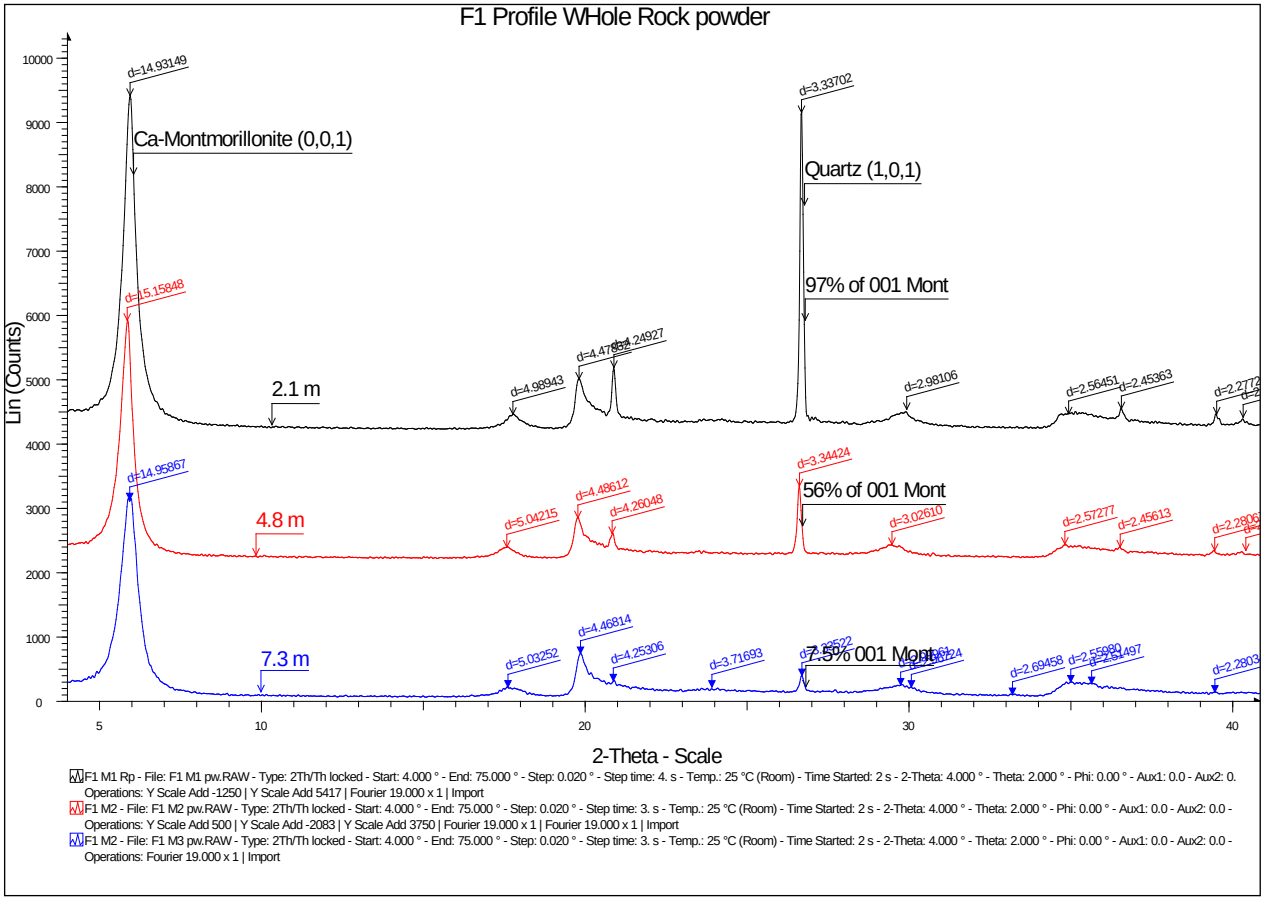

Figure 15 - Whole rock XRD traces for the F1 profile as a function of depth.

4.4 - Chemical analysis

Results obtained from XRF chemical analysis are consistent with the trend observed in diffraction patterns as a function of Depth; Table **3** presents a summary of chemical data arranged as in decreasing depth for all profiles. Likewise loss on ignition has a clear tend to increase with increasing depth due to a increasing smectite content and therefore greater weight loss from dehydration and dehydroxylation. Figure 15 presents all values of Loss on Ignition as a function of depth.

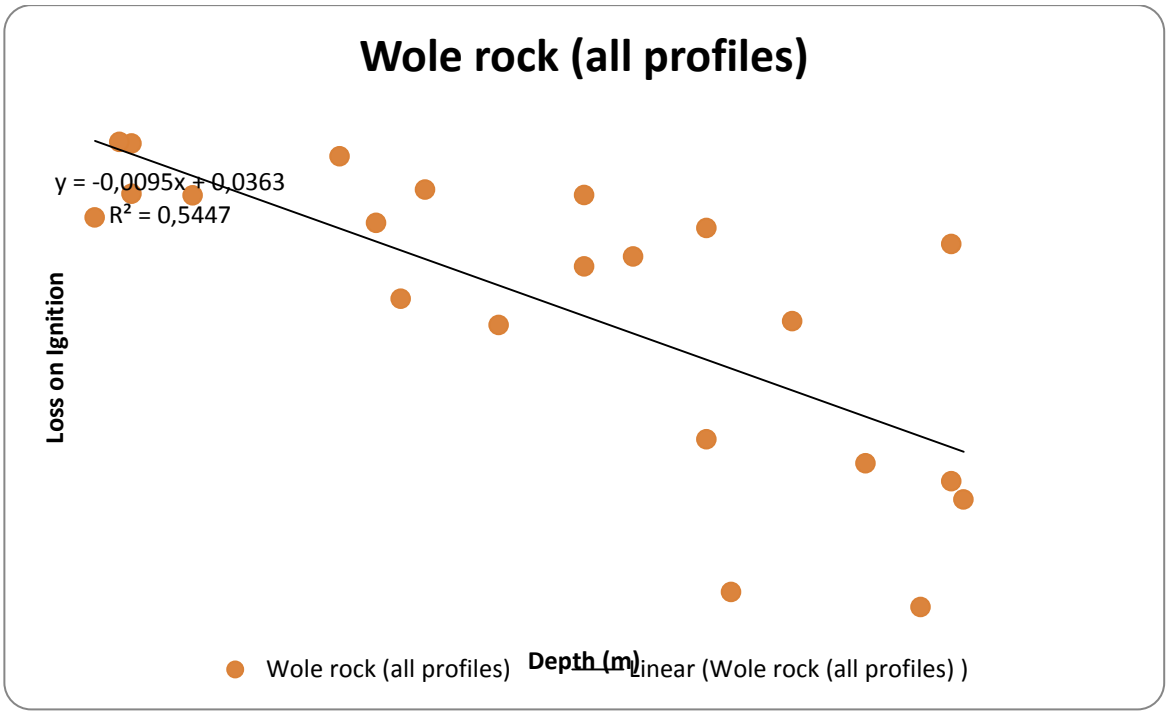

Figure 16 - Loss on Ignition for whole rock samples as a function of depth

Some relevant features observed on chemical analysis results from whole rock lead us to several comclusions about the fluctuations on mineralogical proportions and about the migration of elements thought the profile. We will slighty point them out here and they will be discussed further on in the document.

- Decrease of SiO_2 and increase of Al_2O_3 contents are in accordance with observations in random XRD traces and LOI about increasing clay content as a function of depth.
- Increase of CaO with depth is probably associated with smectite interlayer.
- K_2O and Na_2O both tend to decrease with depth, suggesting that probably there is not a single feldspar phase and they are decreasing as a function of depth, similar to quartz at the expense of Ca –Montmorillonite. We can state that albite and K-feldspar are present in Melo.
- Fe_2O_3 content along the profiles tends to have a non-systematic behaviour, probably due to the presence of some oxides not detected by XRD. There is a general trend to increase with depth, suggesting that it is located basicaly as octahedral substitutions (as Fe^{3+}).
- MgO also tends to increase with depth. It is relatively high along the profile (up to more than 6%). Magnesium is present as octahedral substitution and is perhaps the major factor for high layer charge on all samples.
- Other interesting features can be deduced from TiO_2 being more abundant at the middle of the bed. This feature could have important implications in terms of the known tendency of Ti to be an immobile element and diagenetic characteristics that will be discussed later on.

- P_2O_5 is present in very low amounts and located only in boreholes B and C. If these locations are plotted on the base map with respect to the other two sampling locations, one can notice that these two samples are located in the middle, whereas F1 and F2 are in the northwest boundaries of the occurrence. The same trend was observed in chemical analyses of the <1µm size fractions.

SAMPLE	Na_2O (%)	MgO (%)	K_2O (%)	CaO (%)	TiO_2 (%)	MnO (%)	Fe_2O_3 (%)	Al_2O_3 (%)	SiO_2 (%)	P_2O_5 (%)	SUME	L.O.I.
F1M1	1,68	4,05	0,24	2,54	0,17	0,22	2,68	15,30	60,59	0,00	96,92	9,45
F1M2	1,54	4,56	0,10	2,98	0,10	0,14	2,47	17,36	60,13	0,00	99,90	10,51
F1M3	1,04	5,03	0,22	2,99	0,12	0,06	2,67	17,85	58,88	0,00	98,89	10,03
F2M1	2,96	2,71	1,35	1,35	0,18	0,02	1,38	11,24	74,47	0,00	99,97	4,31
F2M2	2,98	2,53	1,09	1,44	0,20	0,01	1,43	12,09	73,58	0,00	100,04	4,70
F2M3	1,98	3,94	0,51	2,17	0,13	0,02	2,04	15,10	65,73	0,00	99,39	7,78
F2M4	0,00	4,50	0,21	2,54	0,12	0,17	2,38	16,60	61,23	0,00	97,56	9,80
F2M5	0,00	4,43	0,11	2,50	0,14	0,19	2,30	16,07	63,15	0,00	97,84	8,97
F2M6	0,00	5,02	0,13	2,57	0,09	0,10	2,52	16,67	60,22	0,00	97,96	10,63
F2M7	0,00	5,37	0,08	2,62	0,11	0,20	2,74	17,33	58,46	0,00	98,25	11,36
F2M8	0,00	5,42	0,08	2,62	0,08	0,21	2,87	17,66	58,92	0,00	98,37	10,51
F2M9	0,00	5,92	0,20	2,74	0,13	0,03	3,08	17,90	57,77	0,00	98,31	10,54
B1,75	3,67	1,40	1,75	1,17	0,16	0,01	0,80	8,40	80,88	0,22	100,03	1,58
B3,3	3,73	1,49	1,62	1,08	0,16	0,01	0,77	7,69	80,32	0,18	98,96	1,91
B5,2	2,30	3,27	1,22	1,92	0,22	0,03	3,09	14,67	64,74	0,00	99,15	7,70
B6,2	1,83	3,30	0,42	1,96	0,12	0,13	2,27	13,37	61,86	0,00	95,16	9,91
B8,2	1,49	3,59	0,63	1,87	0,09	0,11	1,66	13,56	64,49	0,00	99,13	11,63
C1,4	3,65	1,61	1,63	0,80	0,16	0,01	0,81	8,34	78,77	0,00	99,70	3,91
C3,5	2,82	2,60	1,14	1,42	0,20	0,01	0,97	11,28	74,20	0,00	99,86	5,22
C4,1	0,00	6,23	0,30	2,03	0,14	0,03	2,63	16,68	61,05	0,95	99,23	9,18
C6,0	1,46	3,73	0,12	2,18	0,07	0,07	1,63	13,49	68,63	0,00	99,64	8,26
C8,3	0,00	5,14	0,14	2,74	0,09	0,03	2,74	17,78	57,81	0,00	98,14	11,67

Table 3 . X-ray Fluorescence Chemical analysis of whole rock samples, arranged as a function of depth.

4.5 - Heavy minerals and Geological overview

In order to gather information about the whole diagenetic environment of Bañado de Medina Bentonites, we have separated the particle size between 53 µm and 100µm by wet sieving to observe heavy minerals and overall morphology. Observations were performed by SEM and by petrographic analysis using optical microscopy The following sequence of images resume what was found.

SEM photo showing typical smectite flaky texture of smectite aggregates	SEM photo showing a group of aggregates coated with smectite	SEM photo showing spherical Opal-CT crystal aggregate,

	flakes and also a rounded shape detailed in next figure.	indicative of volcanic origin.
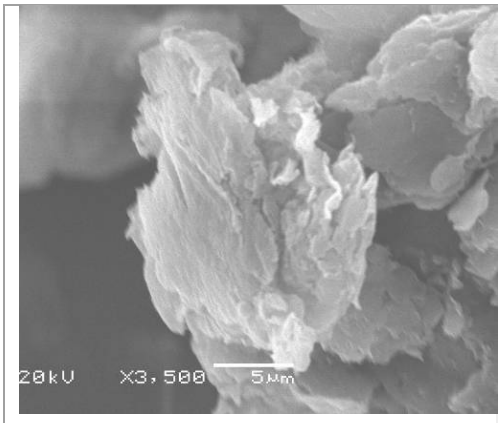	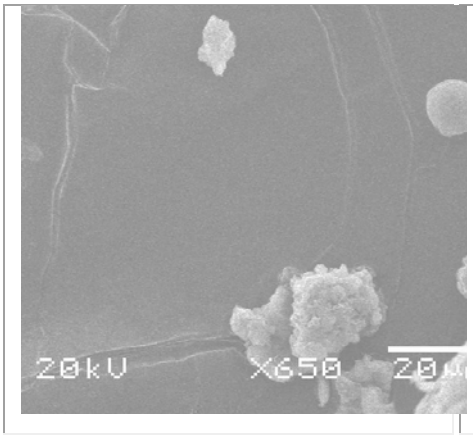	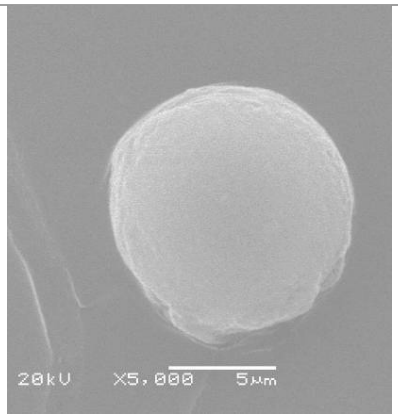
Opal-CT spherules. These textures are rather common, particularly in the high montmorillonitic levels of the bentonite (polarized microscope crossed polars).	Typical textures of devitrified glass; quartz may form keeping the original appearance.(polarized microscope plane polarized light).	A view of a series of Opal-CT manifestation surrounded by a very particular set of grains to give an idea of the grain size distribution and shapes.
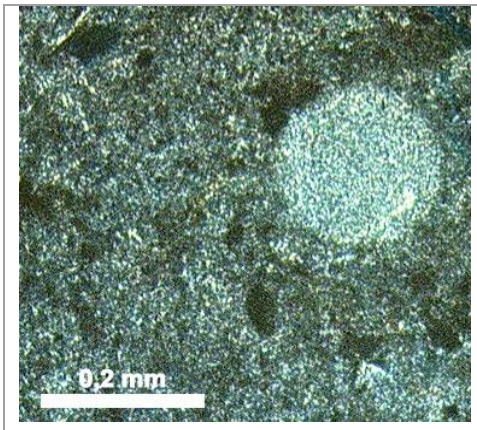	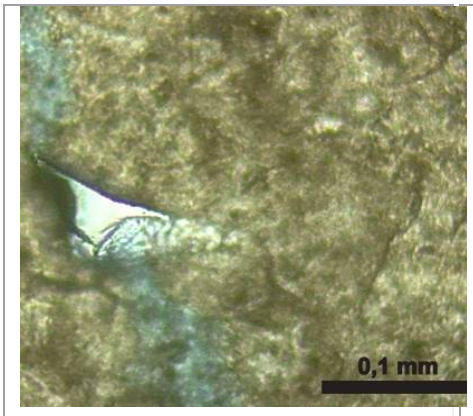	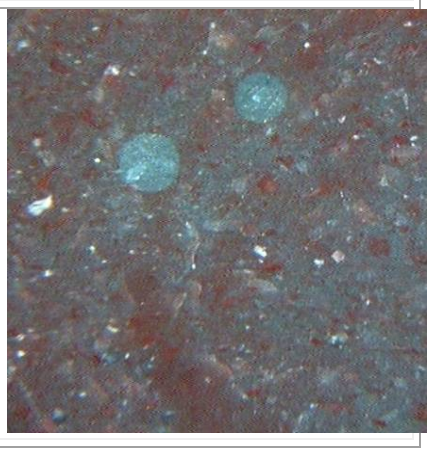

Figure 17 Observed features on SEM and Optical Microscope. The observed spherulitic textures are typical for devitrified volcanic glass glass. Although opal-CT was not detected in XRD traces the characteristic spherulitic textures probably belonged originally to opal-CT which was replaced by recrystallization to quartz, or very unlikely but possibly, it is still is preserved but in small amounts.

Either opal-CT or quartz may form from crystallization of the volcanic glass. That means that the quartz present in the deposit could have been derived either from opal-CT or could have been formed directly from divitrification of volcanic glass.

4.6 -Layer charge estimation and spatial variations

The first method applied was the Christidis Eberl method, which uses the LayerCharge computer program (Christidis & Eberl, 2003), as explained in “materials and methods”

section. The XRD patterns of potassium saturated, ethylene glycol solvated traces was compared to XRD simulated traces calculated from three component interlayering.

4.6.1 – XRD traces

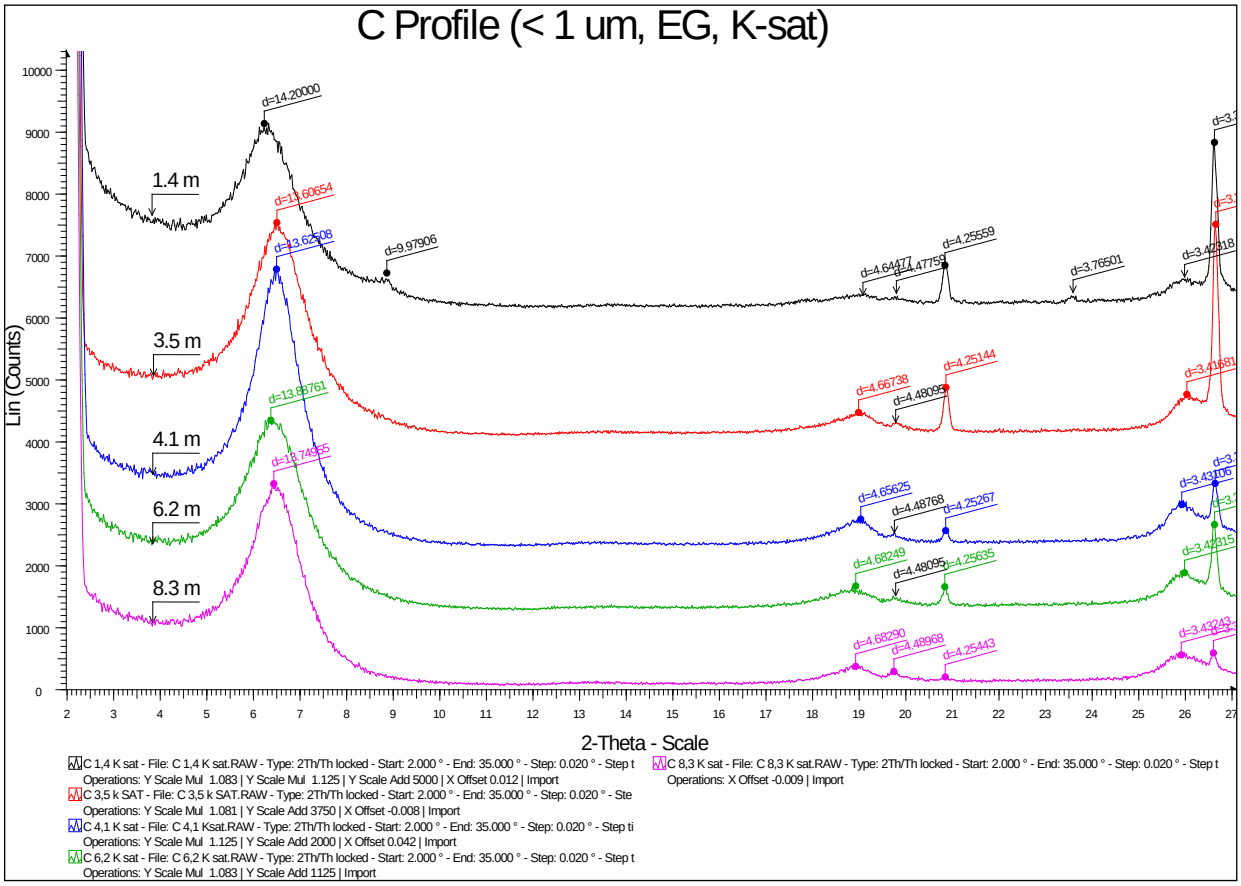

Figure 18- XRD of C profile> 1 μm fraction as specified in the method.

Samples were prepared in batches of 5 at a time to avoid ethylene glycol evaporation before X-ray diffraction, and the 005 smectite reflection was used as a tracer for efficient glycolation. This represents a key factor when trying to fit profiles on the Layer Charge software used to calculate layer charge.

In Figure 18 the overall tendency of layer charge as a function of depth is not very clear. Therefore the Figure 19 zooms on the area where the largest smectite peak appears to remark the trend to decrease layer charge on top and bottom of the deposit or in other words to increase in the middle.

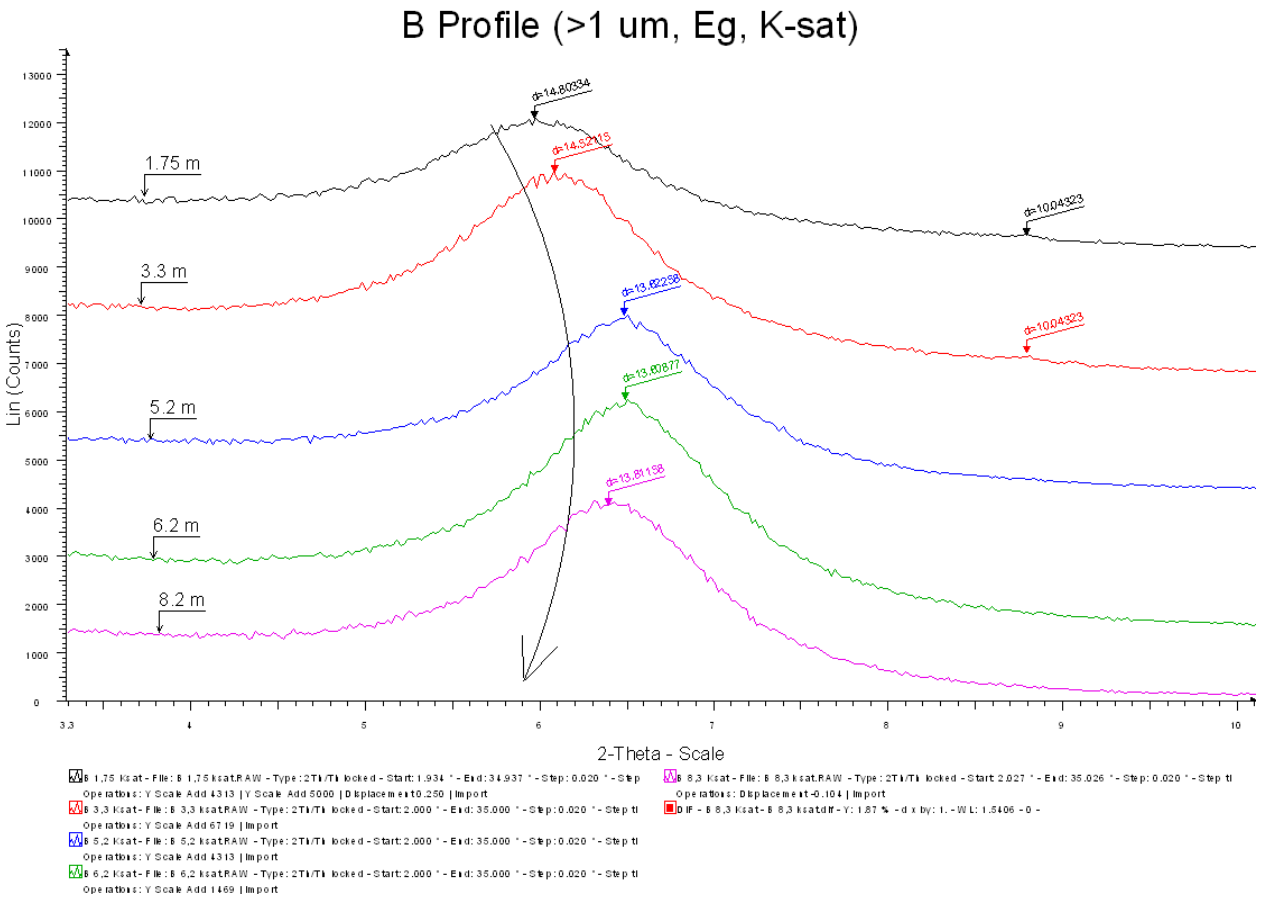

Figure 19 - D spacing variations of the 001 peak poison on B profile as a function of Depth.

The Christidis & Eberl (2003) approach, offers two ways to estimate layer charge, the whole pattern method and the peak position method. In this research we have applied both methods and used the average as the definite result. As a general rule we have established that these values are in general in good agreement although it was noted that for layer charge greater than 0.51 e/huc this was not always the case. Therefore in a general way, if the spread between the two values is above 45% of the whole dispersion on the range of values from all profiles, then the best fit was selected.

Profile		001 Position	Smct. 005	layer charge		
F1	sample	Depth	K-sat	001 rel. intensity	Whole Pattern	Peak Position	**AV.**
	F1M1	2.1	13.23	9%	0.53	0.51	**0.52**
	F1M2	4.8	13.55	16%	0.49	0.49	**0.49**
	F1M3	7.3	13.22	14%	0.49	0.51	**0.5**
F2	F2M1	1.5	13.4	8%	0.51	0.55	**0.53**
	F2M2	1.75	13.9	11%	0.46	0.44	**0.45**
	F2M3	2.5	13.62	16%	0.51	0.56	**0.535**
	F2M4	3.1	13.79	12%	0.53	0.56	**0.545**
	F2M5	4	13.74	16%	0.53	0.53	**0.53**
	F2M6	5.5	13.77	13%	0.53	0.49	**0.51**
	F2M7	6	13.76	12%	0.49	0.53	**0.51**
	F2M8	7.5	14.08	9%	0.53	0.47	**0.5**
	F2M9	8.3	13.9	10%	0.47	0.44	**0.455**
B	B1,75		14.8	15%	0.44	0.41	**0.425**
	3.4B3,3		14.52	20%	0.45	0.47	**0.46**
	B5,2		13.62	21%	0.51	0.49	**0.5**
	B6,2		13.61	23%	0.53	0.44	**0.485**
	B8,2		13.81	21%	0.51	0.44	**0.475**
C	C1,4		14.2	11%	0.46	0.45	**0.455**
	C3,5		13.61	16%	0.49	0.47	**0.48**
	C4,1		13.62	16%	0.53	0.56	**0.545**
	C6,0		13.89	15%	0.56	0.56	**0.56**
	C8,3		13.75	14%	0.47	0.56	**0.515**

Table 4 - Resume of results from layer charge calculations according to the Christidis & Eberl (2003) method. The smectite 005 peak at ca 3.4 Å was used as an indicator of efficient glycol solvation.

From these values we can plot directly layer charge vs. depth to detect any cryptic variation of layer charge in terms of its spatial distribution. It is observed that 3 profiles showed a very clear tendency for increase of layer charge towards the middle of the bed. Only profile 1 behaves differently having values almost constant along the profile. Nevertheless it is necessary to explain that Profile F1 consists only of three samples, and they were taken from the mining front that has been exposed to weathering. For these two reasons the profile is the least reliable source of information.

The following sequence of three graphs presents the clear and repeated trend of layer charge distribution mentioned before

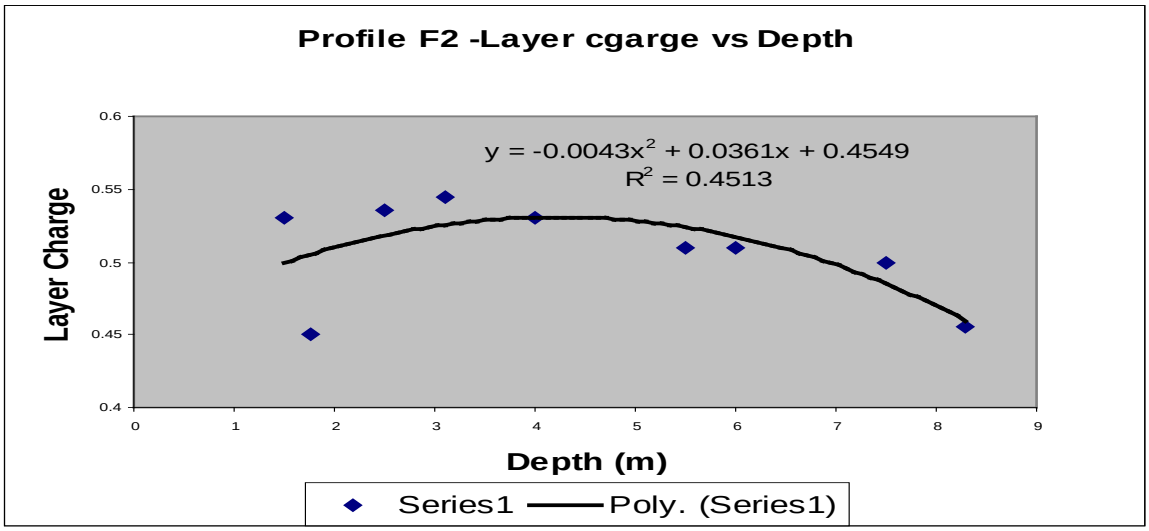

Figure 20 - Layer charge on profile F2 as a function of Depth.

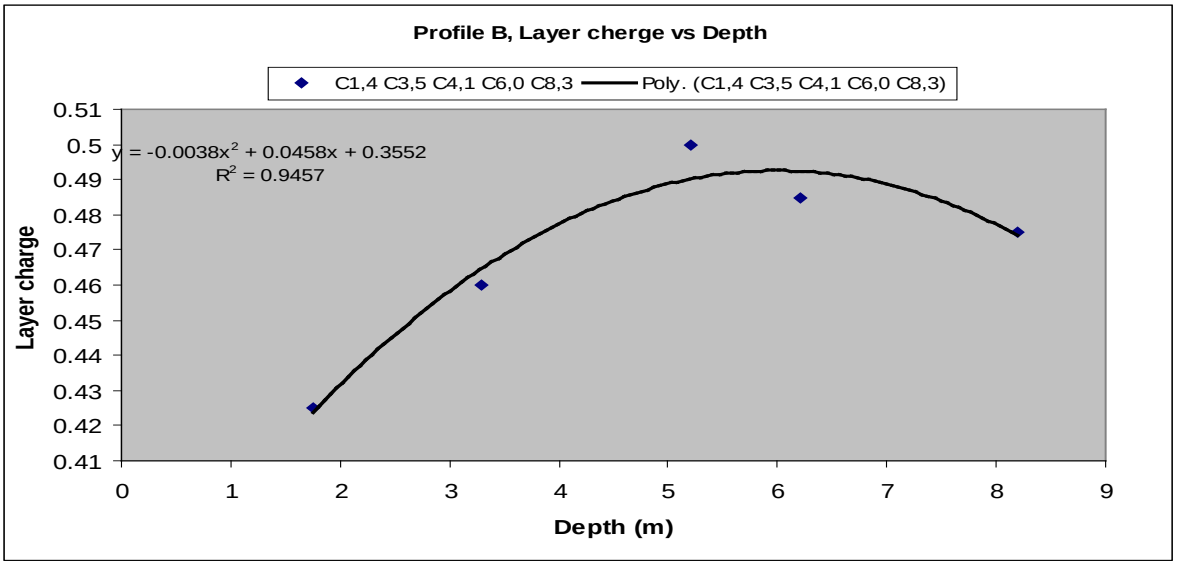

Figure 21 - Layer charge on profile B as a function of Depth.

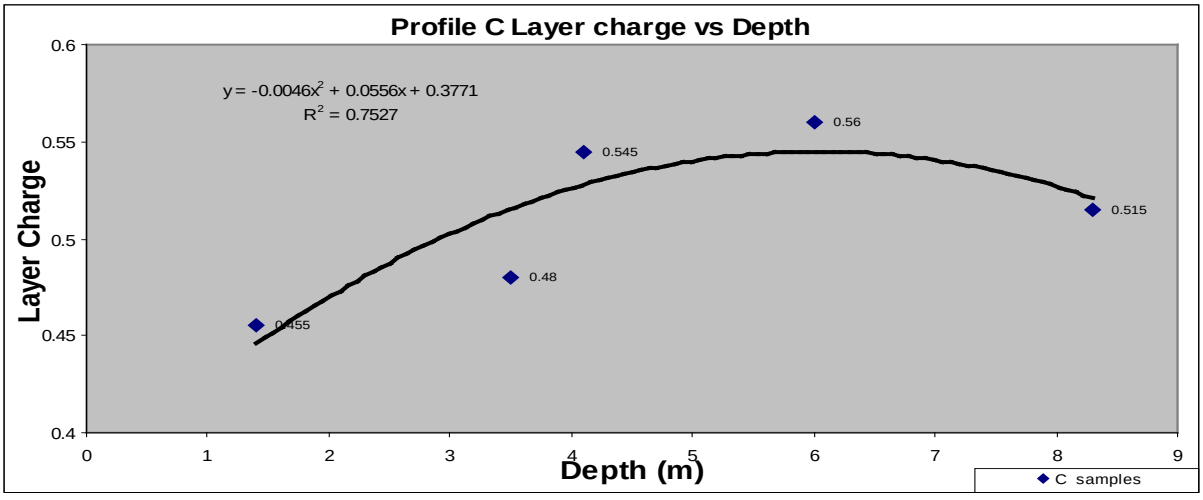

Figure 22 - Layer charge on profile C as a function of Depth.

4.5.2 – Spatial distribution of layer charge

Using the same graphical inferences as those used in "the spatial distribution of samples", we present a graph with a color scale to illustrate the spatial distribution of layer charge according to the average values obtained for all samples from they're XRD traces.

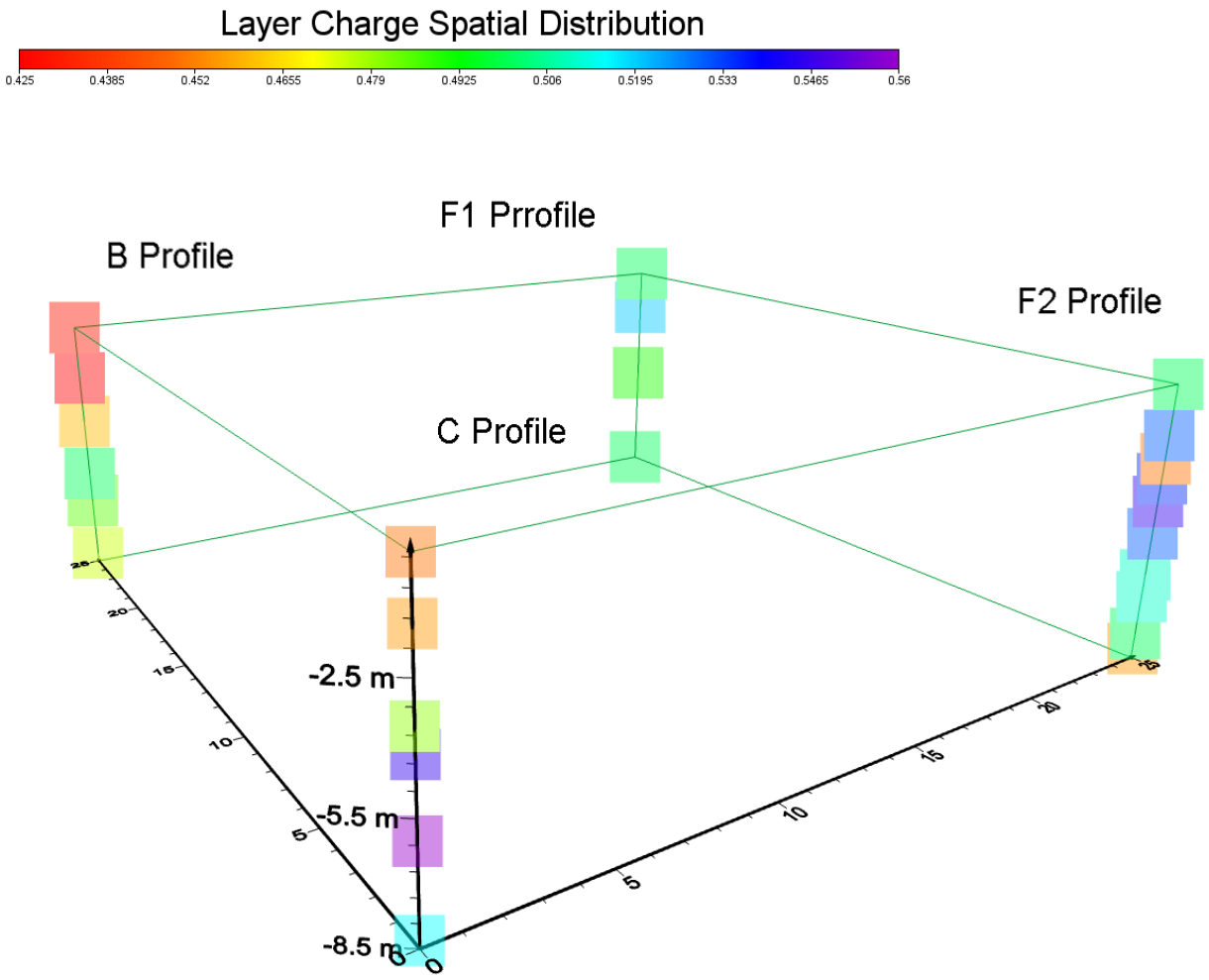

Figure 23 – 3D model of spatial distribution of layer charge.

We also made an attempt to develop a volume model. Nevertheless the data was not sufficient to provide with a satisfying representation. The software used was Golden Softer Voxler 3 and it interpolates also in three dimensions, linearly in this case. In the present study we considered only a small area surrounding the axes; hence the graphical representation approaches reality.

It is important also to distinguish that values for layer charge obtained from borehole samples[13] seem to have a more coherent behavior in terms of rational evolution along the profiles.

[13] Profiles B and C. F1 and F2 correspond to fresh cut samples on mining fronts.

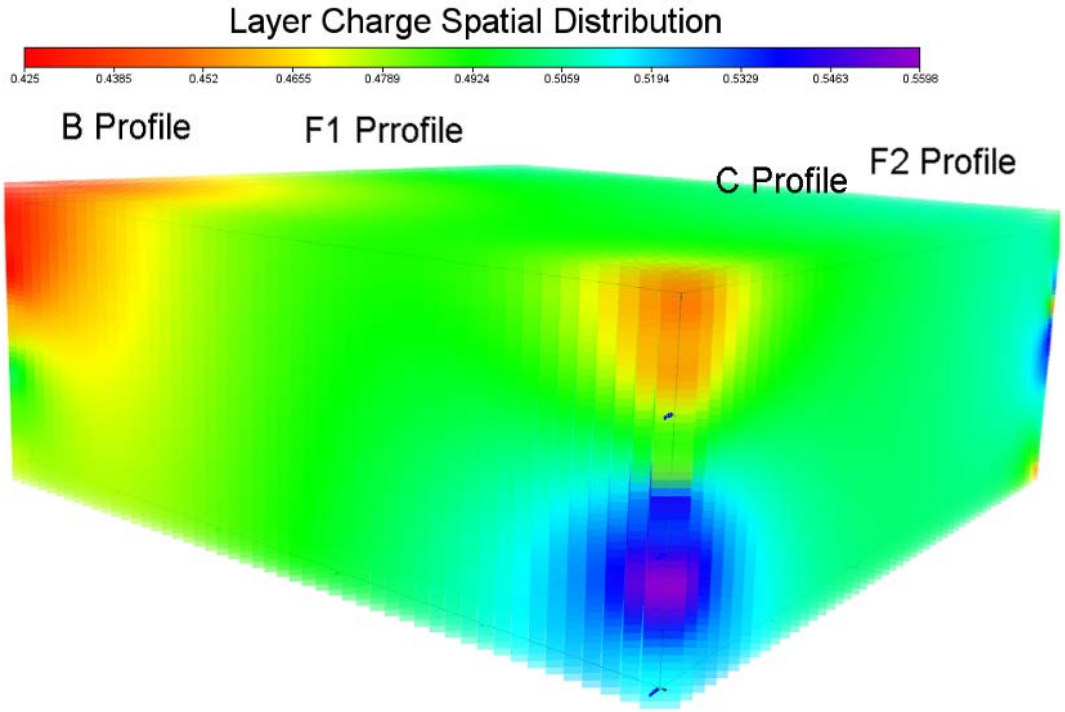

Figure 24 – Volumetric perspective of spatial distribution of layer charge (Profiles B, C and F2)

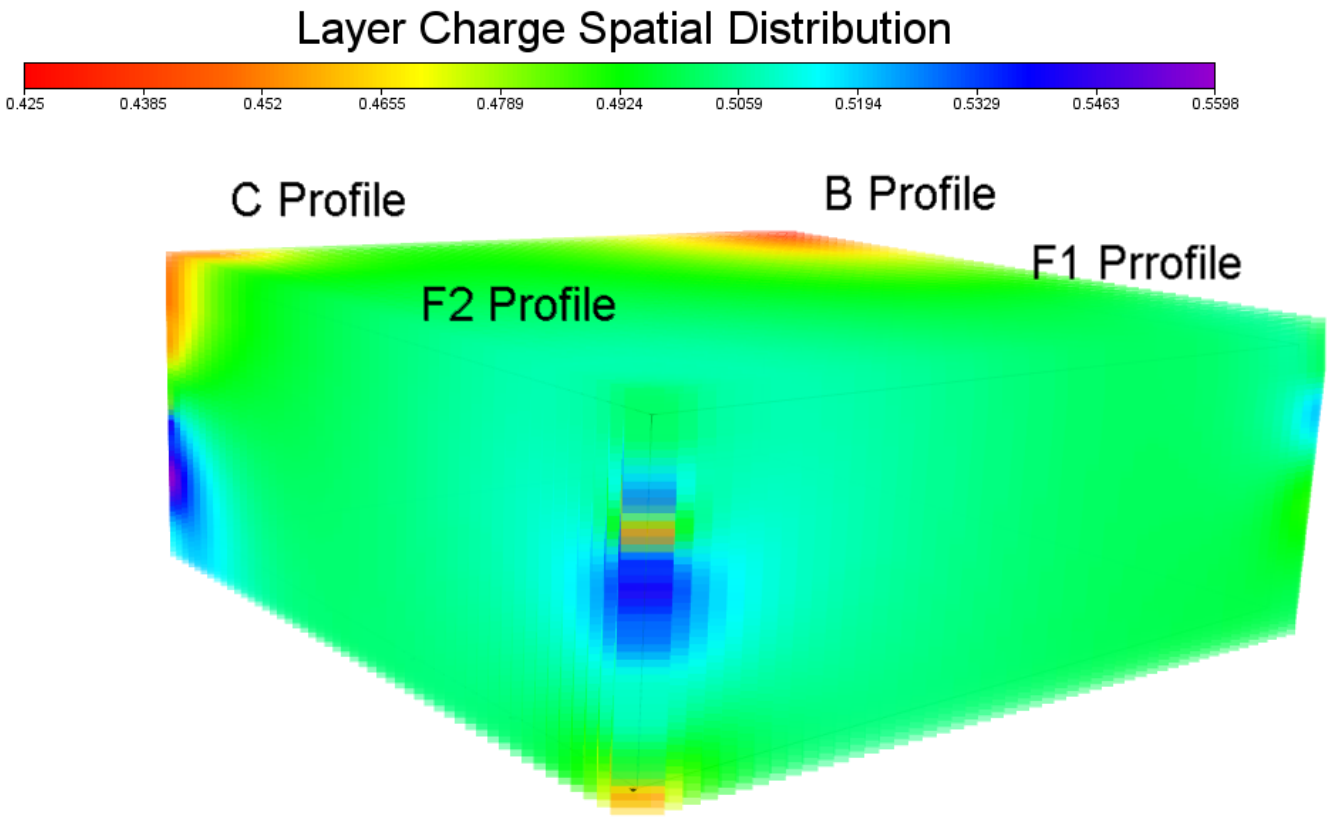

Figure 25 – Volumetric perspective of spatial distribution of layer charge(Profiles F2,F1,C and F2)

4.6.3 – Layer charge calculations by the Structural Formula (SF) Method

As it was already explained before, the SF method of layer charge calculation will be used to corroborate the trends observed with the first method and also to be able to approach the nature and amount of isomorphic substitutions that could help us to understand how layer charge diverges spatially.

For this task the main Input is chemical analysis of the <1µm size fraction acquired with XRF.

Sample	MgO (%)	K_2O (%)	CaO (%)	TiO_2 (%)	MnO (%)	Fe_2O_3 (%)	Al_2O_3 (%)	SiO_2 (%)	P_2O_5 (%)	SUME	LOI
F1M1	4.83	0.00	2.70	0.18	0.23	3.60	18.63	64.72	0.00	97.94	**11.8%**
F1M2	4.95	0.17	2.77	0.12	0.15	2.89	19.53	69.52	0.00	100.10	**10.7%**
F1M3	4.93	0.15	2.59	0.13	0.10	3.02	17.12	59.70	0.00	90.47	**11.6%**
F2M1	3.36	0.88	1.53	0.18	0.02	2.10	13.83	70.50	0.00	95.54	**7.0%**
F2M2	3.35	0.52	1.53	0.21	0.01	2.12	15.75	71.14	0.00	97.81	**8.2%**
F2M3	4.26	0.20	2.11	0.10	0.01	2.01	16.03	70.51	0.00	98.03	**9.1%**
F2M4	4.73	0.14	2.25	0.10	0.23	2.50	17.41	66.54	0.00	96.69	**11.7%**
F2M5	4.91	0.00	2.43	0.08	0.14	2.66	16.96	68.27	0.00	95.45	**9.6%**
F2M6	4.72	0.08	2.34	0.10	0.12	2.90	17.56	66.57	0.00	94.38	**10.6%**
F2M7	5.27	0.00	2.53	0.10	0.11	3.01	18.23	65.93	0.00	95.17	**11.4%**
F2M8	5.19	0.00	2.55	0.09	0.38	2.81	18.92	65.61	0.00	98.26	**12.0%**
F2M9	5.59	0.00	2.65	0.13	0.03	3.53	19.21	64.13	0.00	97.97	**14.0%**
B1,75	3.00	1.04	2.29	0.23	0.03	2.25	14.88	70.74	0.41	98.34	**6.8%**
B3,3	3.50	0.93	2.23	0.20	0.01	1.99	16.27	70.31	0.24	99.05	**7.1%**
B5,2	5.18	0.34	2.38	0.18	0.03	4.27	20.28	62.97	0.00	95.63	**10.1%**
B6,2	5.25	0.00	2.38	0.09	0.11	2.79	19.16	66.38	0.00	96.16	**10.6%**
B8,2	5.71	0.11	2.52	0.09	0.14	2.95	19.80	67.85	0.00	101.59	**11.5%**
C1,4	3.42	1.60	1.46	0.35	0.02	2.63	16.69	69.87	0.00	99.25	**7.6%**
C3,5	3.94	0.28	2.14	0.12	0.01	1.23	16.67	70.77	0.00	98.37	**14.3%**
C4,1	4.99	0.00	2.60	0.11	0.04	3.17	18.40	65.81	0.00	95.12	**10.9%**
C6,0	5.06	0.00	2.43	0.08	0.11	2.48	18.16	66.87	0.00	97.78	**10.8%**
C8,3	5.71	0.12	2.60	0.08	0.04	2.83	18.97	65.15	0.00	97.86	**12.6%**

Table 5- XRF Chemical analysis results for <1um size fraction for all samples.

Quartz in excess observed on XRD < 1 µm fraction is rather frequent in this samples. To avoid overestimation of SiO_2 in the structural formula calculation, a semi quantitative method was used to establish roughly quartz content and this amount was subtracted from the initial chemical composition. Table 6 shows the quartz content on the < 1 µm size fraction as a function of depth in profile C.

4.7 - Organophilization & Cation Exchange Capacity

Cation exchange capacity was estimated to determine the proportion of amine that shall be used in the procedure. The amount of dodecylammonium Chloride ($C_{12}H_{28}ClN$)that will be used should be 1 to 1.5 time the CEC value, It was calculated by ammonium acetate method and some results are shown in table 8

Sample	Layer Charge	C.E.C	Depth
F2M1	0.55	116.3923	2.1
C1,4	0.45	104.8356	1.4
C3,5	0.47	86.34495	3.5
C4,1	0.56	100.1304	4.1
C6,0	0.56	106.3215	6
B6,2	0.44	98.51249	6.2

Table 6 – Cation exchange capacity for random samples

It is well known that C.E.C should be directly proportional to layer charge. The following figure plots six values of C.E.C calculated as a function of their layer charge to try and observe the classic correlation.

Figure 26 – Cation exchange Capacity vs. Layer charge.

From the graph we can observe an evident tendency to have two well defined groups in the universe of samples plotted. Enclosed by the red circle, one can see samples

ranging low values of CEC and Layer charge too; the blue one encloses the opposite group having High CEC and Layer charge.

After organophilization took place, controlling all variables in order to assure that the same conditions repeated for all samples. Oriented slides were prepared on methanol solution and after dried they were kept in a desiccator to avoid moisture adsorption until X-Ray diffraction.

Once in diffraction our only interest was to find out 001 d-spacings of all samples and to determine if there was any influence of layer charge on this. Diffraction range was set from 2º theta to 20º theta for the 001 reflection peak would be enough to gather conclusions about dodecylammonium Chloride intercalation. Figure 27presents several diffraction patterns on oriented slide for a single sample to have a comparative overview.

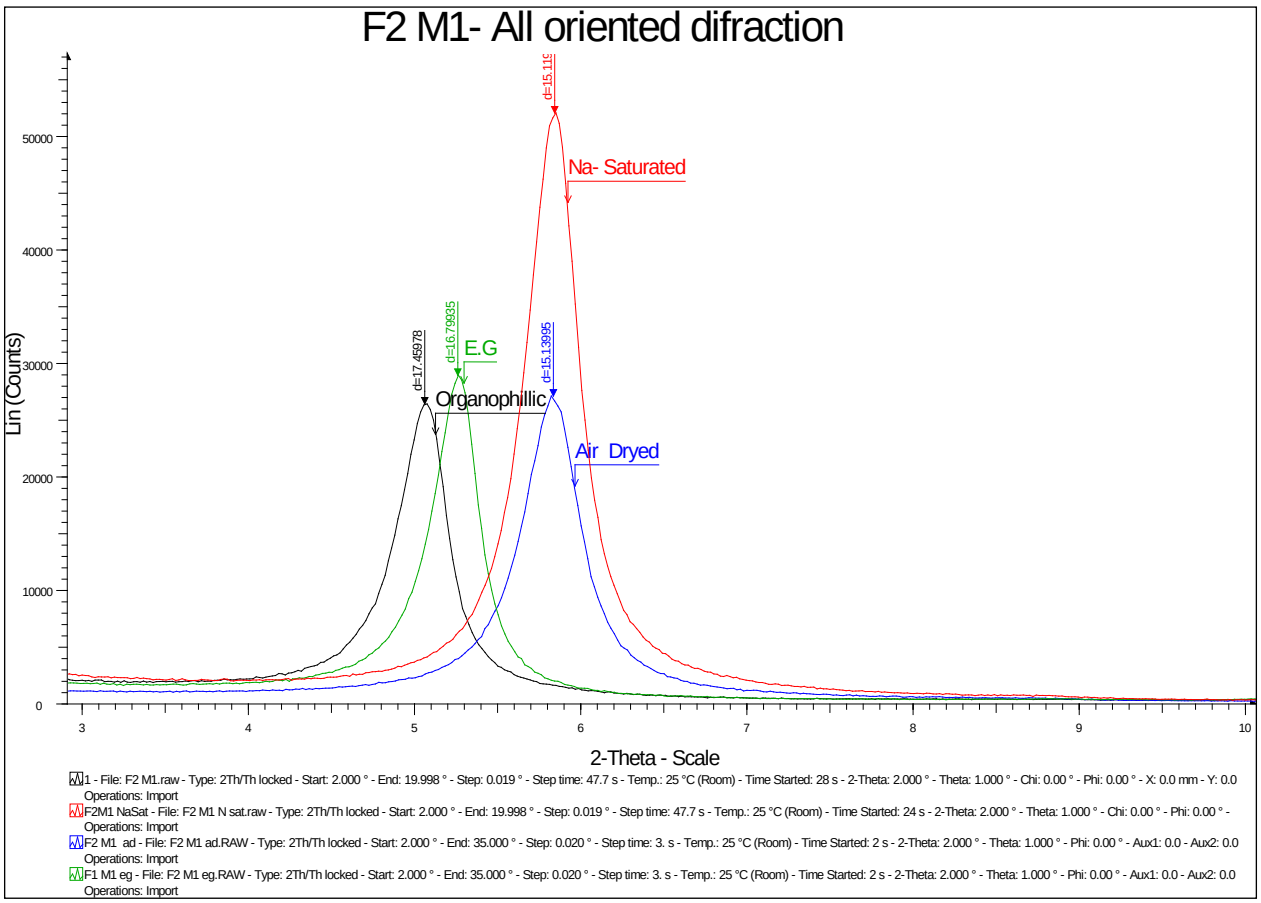

Figure 27 - Sample F2M1 Oriented slide diffractions for air dried, Na- saturated, ethylene glycol solvated and organo clay intercalated with dodecylammonium chloride ($C_{12}H_{28}ClN$).

A normal expansion from air dried to ethylene glycol treated sample of 1.5 Å, expandability corresponding to 2EG-EG. As for the Organophilic clay expandability, the

peak at 17,46 Å is characteristic of a Bilayer amine intercalation, nevertheless this issue will be largely discussed in next chapter.

At a first glance, all Organophilic xrd patterns show a similar expandability in terms of they're 001 ($C_{12}H_{28}ClN$)-Montmorillonite peak position, ranging from 17,05 Å To 17,68 Å. They could all be considered as bilayer sorbed Organoclay according size of the alkyl chain used, and the known sorption isotherm (Boyd and Jaynes, 1994).

Despite the slight d-spacing differences among samples, there is a well defined positive relationship between layer charge and position of the 001 peak of the organofilic smectites. This is a clear indication that the position of the 001 peak is related to the magnitude of layer charge.

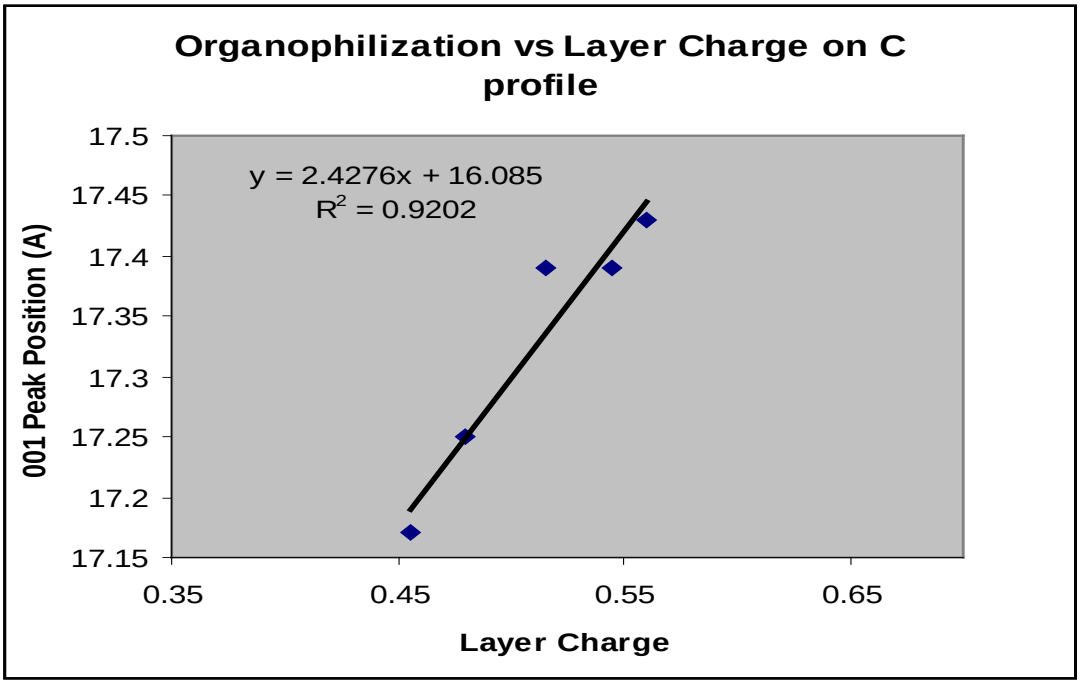

Figure 28 - Organophilic 001 peak position for C profile as a function of layer charge.

An interesting trend was observed when the peak position was plotted vs depth; the d-spacing increases towards middle of the Bentonite bed, and decreasing again towards the bottom, similar to the variation of layer charge, exhibited on Fig. 29.

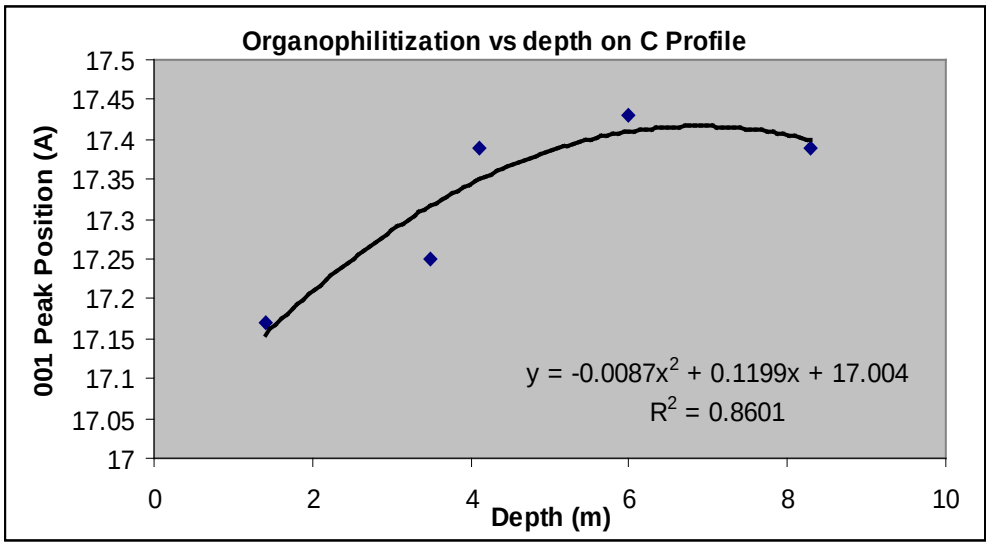

Figure 29 - 001 peak position for Organophilic C profile as a function of depth

Perhaps the most representative evidence of Organophilicity efficiency with respect to layer charge spatial distribution, is given the a comparative analysis presented as follows from whole Profile C, amine intercalated 001 peak area analysis and it's evolution with depth.

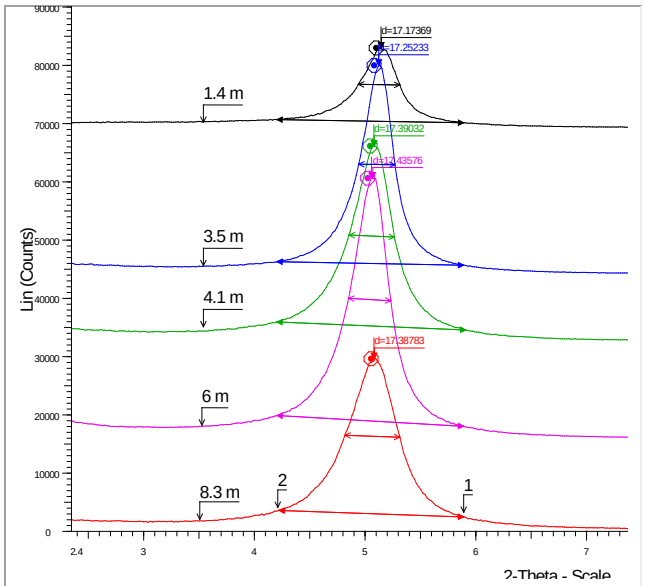

XRD traces of Organophilic C-Profile

Raw 001 peak Area after Organophilization as a function of Depth for Profile C (cps x deg)	Net Peak Area after Organophilization as a function of Depth for Profile C (cps x deg)
2620.6	121.3
1930.7	299.2
1593.3	330.2
1082.7	413.9
418.8	317.2

Figure 30 – Relative Area evolution of the amine intercalated 001 montmorillonite Peak as a function of Depth for Profile C.

Relative area of diffraction peaks is a very common technique used normally to obtain information about relative proportions of mineral phases present in a multimineralic sample. In our case we assume that is pure smectite interacting with dodecylammonium Chloride under the same conditions for all samples, even if quartz could be present in the < 1 μm oriented slides as it was observed in the XRD traces for this size fraction, we

assume that it does not affect with the process, for all key thermodynamic parameters[14] where controlled along the Organophilization procedure.

Figure 31 shows on the right side a series or peak areas as a function of depth, the numbers labeled 1 and two where the referential points to establish the same area limits on all samples for profile C. For this purpose we used the area estimation tool offered by EVA diffraction analyzer software, The following figures display the well expressed correlation between layer charge and degree of organophilization. The results will be discussed in the next chapter.

To express the perfect correlation between layer charge spatial distribution values and the grade of Organophilization we present figure 31 that will be commented in detail on the discussion chapter.

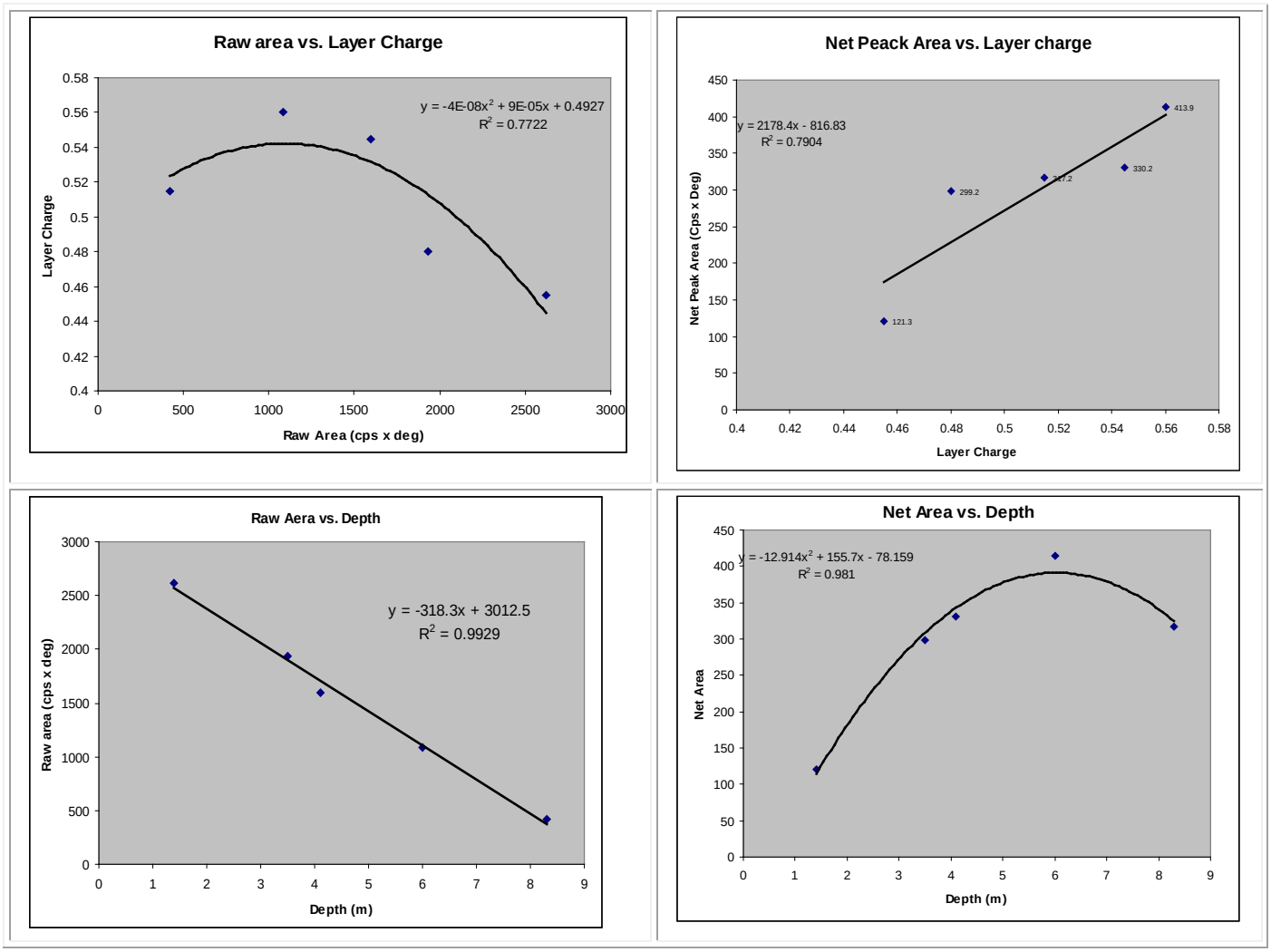

Figure 31- Organophilic 001 peak area Evolution as a function of Depth & Layer charge.

[14] Ph was kept around 6,75 and aging temperature was not more than 60º C.

Chapter V
Discussion of results

5.1 -Regarding Geological observations

Bañado de Medina represents a very rear opportunity to study a bentonite deposit that seems to be unaffected since the early Permian in order to observe alteration features that may have influenced all physical and chemical properties of the smectites present. As it has been stated before in other investigations, we found evidence of a rhyolitic to Dacidic volcanic source from opal-CT and quartz texture. To approach the question of preservation conditions we accept the fact that e geological context linked to a intracratonic basin (Paraná Basin) was dominated by a rather low diagenetic conditions, a maximum temp of around 55 ºC was estimated from vitrinite analyses of a coal Bed that belongs to Rio Bonito formation(L. Calarge et al 2001). However, this is not sufficient to explain neither the atypical thickness for a stratiform layer of Bentonite developing from volcanic ash alteration over lagoon to transitional environment that can arise up to almost 6 m or the preservation from erosion, weathering and other surface related degradation processes. If volcanic ashes were so voluminous that in a lagoonal environment a bed of 6 m thickness was formed, then we would have to ask , what happened to the surrounding material derived from this events considering that the volcanic source is located more than 1000 km away?

On the other hand, the spatial evolution on mineralogical composition indicates a clear tends to decrease trace minerals as quartz and feldspar to an increment of magnesium rich dioctahedral montmorillonite which electrical disequilibrium tends to be compensated primarily by Ca+ cations in the interlayer. XRD patterns on whole rock, XRF chemical results and heavy minerals observations and all in agreement with mineralogical proportion evolution as a function of depth. But if this is the case, why is there not a single trace of I/S mixed layer over the top of the deposit where smectite proportions are around 50% of the overall mineral composition and Na is present within Albite. The only evidence of Illite shown on XRD is traces was found at 1.5 m depth having a relatively small refection and clearly pure Illite, what lead's us tu think that it is provably from detrital origins hence transition mixed layered phases are totally absent.

As a consequence we can propose that as a locally, there is a model that can explain all uncertainties expressed before by means of structural and mineralogical arguments registered in this research. We believe that a set of parallel oriented faults described by ALbarnaz et al,2010; had buried part of the original diagenetic bed, hence the deposit at Melo is actually modelled by taking two equally oriented faults as boundaries, above this limits drill bores resulted with no signals of Bentonite. Moreover, It is likely that surrounded overlying Bentonites where then transported and carrying larger content of accessory minerals. This could explain the great thickness of the bed and uneven distribution of mineral phases as a function of depth. It would also explain why this rather small occurrence has preserved for such a long time and surrounded areas that most probably were also containing Bentonite has now been eroded. This hypothesis could set

important prospecting criteria to search for Bentonite occurrences regionally, particularly considering the large distance to the volcanic ash source.

5.2 -Regarding layer charge spatial distribution, heterogeneity and nature.

Although this is not the first attempt to interpret how layer charge is distributed over a Bentonite deposit (Christidis & Warren Huff, 2009) in order to correlate this behavior to formation characteristics, it is probably the first time that the layer charge distribution is approached in a tridimensional perspective and it is directly associated with properties like organophilization.

We observed an overall tendency in three of the 4 profiles (18 from the 21 samples analyzed) for layer charge to increase up to values ranging from 0.5 to 0.56 electrons per half formula unit at the middle of the Bed and decrease at the top and bottom to values ranging from 0.46 to 0.49 per half formula unit. It was also in agreement with cation exchange capacity results, in which samples tend to be polarized in two groups when plotting CEC vs. layer charge, one group having CEC 85-100 eq.mol/100g and lower layer charge values, and the other group having CEC 100-120 eq.mol/100g and higher layer charge values.

Furthermore, the < 1 µm size fractions are characterized by higher Mg and Al contents as a function of depth, both cations being present mostly in octahedral sites. However the rate of increase of Al with depth is greater than the remaining octahedral located cations. This would affect gradually the magnitude and distribution of layer charge as was observed along the research.

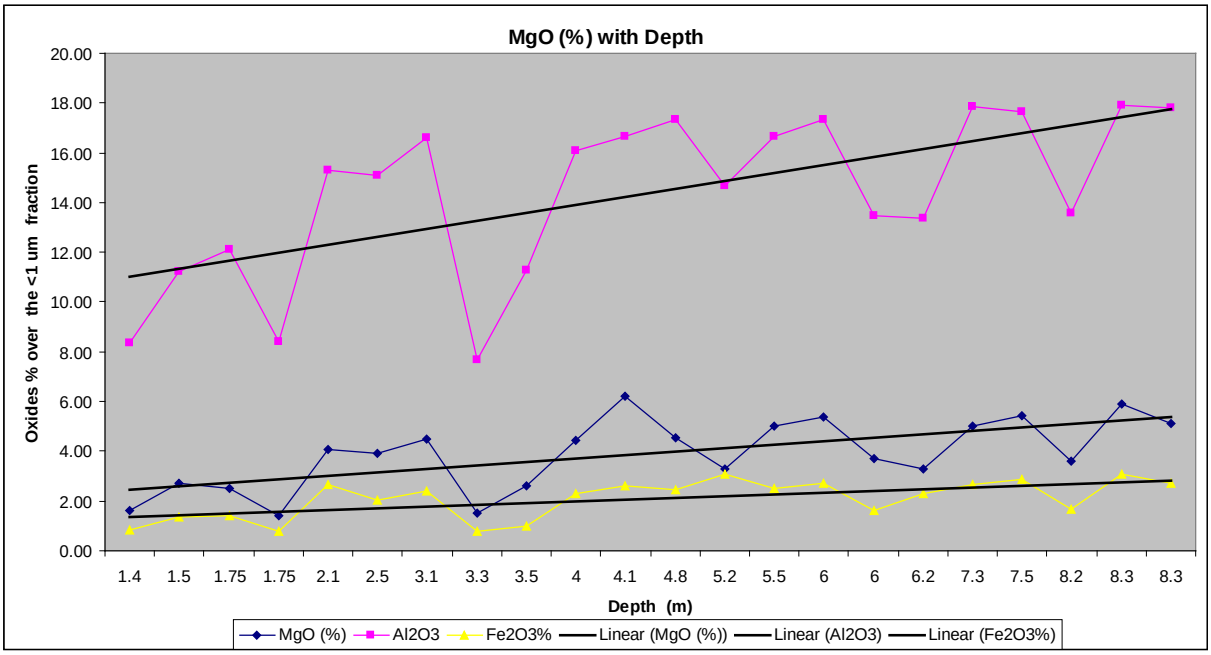

Figure 32 – Mayor Cations affecting layer charge as a function of Depth.

he fact that the Bentonite bed is placed over a sandstone layer could have created alteration conditions in which the water/ rock ratio along the profile would form a greater number of octahedral substitutions in the middle of the deposit and consequently higher layer charge.

Profile P1 did not have a coherent behavior compared to the other three profiles, perhaps because samples were obtained from the oldest exposed mining front; only three samples were taken from this location and although the layer charge values were on the same range we did not observe the same systematic trend with depth. As a general remark we can outline that results over the boreholes were largely more consistent than the ones obtained over fresh cut samples on mining fronts.

5.3 - Regarding Organophilization and physical properties

All Organophilic XRD patterns showed a similar d-spacing of the 001 ($C_{12}H_{28}ClN$)-Montmorillonite complex, ranging from 17,05 Å to 17,68 Å. They could all be considered as bilayer complexes according to the size of the alkyl chain used, and the known sorption isotherm (Boyd and James, 1994).

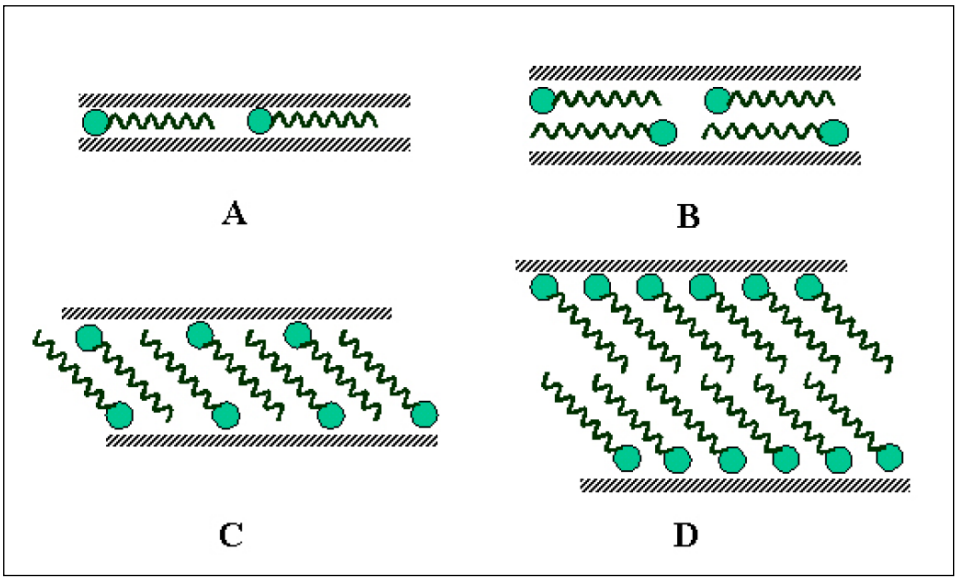

Figure 33 – Arrangement of Alkylammonium ions in mica-type silicates with different layer charges. A) Lateral Monolayer, B) Lateral Bilayer, C) Paraffin-type monolayer and D) Paraffin type bilayer.

The basal spacing for each type of intercalation can be described as step wise. Inr mono-bilayer transitions with samples having layer charge heterogeneity the transition can occur over a range of alkylammonium carbon chain length rather than in a single discrete step (Figure33).

Following this principles we were able to establish a linear trend on the XRD traces of ($C_{12}H_{28}ClN$)-smectite, between the 001 d-spacing of the organophilic smectites and the layer charge estimated prior to organophilization. Similar trend was observed between the layer charge and the net and raw peak areas of the resulting organophilic clays. Consequently we can expect that layer charge spatial distribution could have important influence on the quality of interaction of bentonites not only when organophilization is intended but for any other application based on physical properties of smectites present in bentonites.

5.4 -Conclusions

1 – Layer charge spatial variation for the Bañado de Medina Bentonite deposit displays a clear tendency to increase at the middle of the bed. We believe that more important than the trend itself it is the fact that diagenetic processes and alteration implicit on Bentonite occurrences, tend to have a gradual cryptic, and rational distribution; directly relative to the formation characteristics and preservation afterwards. To use this mineral resource properly one needs to understand the specific emplacement of and distribution of octahedral and tetrahedral substitutions in smectite structure, for it is layer charge the driven force for all 2:1 phyllosilicates interaction in any application context.
Therefore we could not expect that the tendency of layer charge spatial distribution observed could be extrapolated to other deposits of similar origins, but the basic principles should apply; even more important, by understanding it's own formation context one could predict eventually what kind of layer charge spatial distribution a specific deposit could have.

2 – The hypothesis offered in this document about the local conditions that lead to the preservation of the Melo Bentonite deposit, shall be further studied. Perhaps a way to do so would be simply by analyzing the evolution of heavy minerals and specific textures observed in quartz as a function of depth. Also the distribution of feldspar minerals could help to better understand which prospecting criteria could be used on the task to find similar bentonite occurrences regionally.

3 – A very clear correlation was observed by comparing XRD traces from organoclays, ($C_{12}H_{28}ClN$)-Montmorillonite, with the layer charge values. The most evident organophilicity efficiency as a function of layer charge was established by correlating layer charge spatial distribution with respect to amine intercalated 001 d-spacing peak area analysis. The 001 d-spacing of the organoclay tends to increase with increasing layer charge. The position of the 001 peak ranges between 17.15 Å and 17.5 Å and the raw 001 peak area after organophilization can vary from 2620.6(cps x deg) to 418.8 (cps x deg). They can all be considered as bilayer intercalated complexes. Nevertheless we can expect that the influence of layer charge spatial distribution could have more tangible effect when compared with other applications, such as acid activation or viscosity, because evaluation of results will not be presented over a stepwise expandable behavior typical of amine-clay interactions.

4 – Some direct implications of these results could be applied to actual bentonite mining. It is the usual practice to estimate the quantity of reactants when trying to stimulate cation exchange according to the smectite proportion within the bentonite. Physical parameters like layer charge are considered to be fixed. This new approach would have an impact not only on the way bentonites are treated but also on the way they are mixed after extraction resulting probably in a more homogeneous material if the correct criteria of layer charge spatial variations are used.

5.5 - References

- Ahmetr Mermut and G. Lagaly. Baseline studies of the clay minerals society source, layer-charge determination and characteristics of those minerals containing 2:1 layers Clays and Clay Minerals, Vol. 49, No. 5, 381–386 and Vol. 49, No. 5, 393–397, 2001.
- Albarnaz, L. D. T. A Jazida de Bentonita de Bañado de Medina, Melo, Uruguai: Geologia, Mineralogia e Aplicação Industrial. Porto Alegre: Universidade Federal do Rio Grande do Sul, Instituto de Geociências, 2009.
- Blachier C., L. Michot, I. Bihannic, O. Barrès, A. Jacquet, M. Mosquet , Adsorption of polyamine on clay minerals Journal of Colloid and Interface Science 336 (2009) 599–606
- Bossi, J; Navarro, R. Esquema Preliminar sobre la Evolución Geológica del Uruguay durante el Periodo Cámbrico. Actas X Congresso Geológico Argentino. I: 346 – 350. Tucumán. Argentina. 1987.
- Calarge Liane Maria, Alain Meunier, Milton L.L. Formoso. A bentonite bed in the Acegua´ (RS, Brazil) and Melo (Uruguay) areas: a highly crystallized montmorillonite. Journal of South American Earth Sciences 16 (2003) 187–198
- Calarge L., B. Lanson , A. Meunier, and M. L. Formoso, The smectitic minerals in a Bentonite deposit from Melo (Uruguay). Clay Minerals 38 (1) (2003) 25-34.
- Christidis G.E. (1998), Comparative study of the mobility of major and trace elements during alteration of an andesite and a rhyolite to bentonite, in the islands of Milos and Kimolos, Aegean, Greece. Clays and Clay Minerals 46: 379-399
- Christidis G.E. (2001), Formation and growth of smectites in bentonites: a case study from Kimolos Island, Aegean, Greece. Clays and Clay Minerals 49: 204-215.
- Christidis G. E., D. D. Eberl, Determination of Layer Charge characteristics of smectites, Clays and Clay minerals, Vol 51, No. 6,644-655,2003.
- Czímerov, J. Bujdák, R. Dohrmann, Traditional and novel methods for estimating the layer charge of smectites. Applied Clay Science 34 (2006) 2–13
- Deligiann L., A. Ekonomakou Uses of Organo Clays, Bentonite Division-Silver & Barite Group. (2010).

- Elements magazine, Bentonites versatil clays. Vol 5 number 2, April 2009 issue.
- Malla P. B. , M. Robert, L. A. Douglas, D. Tessier, and S. Komarneni. Charge heterogeneity and nanostructure of 2:1 layer silicates by high-resolution transmission electron microscopy. Clays and Clay Minerals, Vol. 41, No. 4, 412-422, 1993
- Meunier A, D. dani M, , Zahraoui M, Beaufort D, El Wartiti M, Fontaine D, Boukili B, El Mahi B (2005) Clay mineralogy and chemical composition of bentonites from the Gourougou volcanic massif (northeast Morocco). Clays and Clay Minerals 53: 250-26
- Laird D. A., A. D. Scott, and T. E. Fenton. evaluation of the alkylammonium method of determining layer charge 1. Clays and Clay Minerals, Vol. 37, No. 1, 41--46, 1989.
- Murray Haydn H., Clay sorbents: the mineralogy, processing and applications. Acta Geodyn. Geomater., Vol.2, No.2 (138), 131-138, 2005
- Petit S. , D. Righi, J. Madejova and A. Decarreau Layer charge estimation of smectites using infrared spectroscopy, Clay Minerals (1998) 33,579-591
- Kaufhold S., Comparison of methods for the determination of the layer charge density (LCD) of montmorillonites. Applied Clay Science 34 (2006) 14–21
- Pinheiro João Paulo Porto, Isabele Bulhões Aranha, Caracterização cristaloquímica preliminar de bentonitas brasileiras.
- The Clay Mineral Society (CMS). “Workshop lecture Layer charge characteristics of 2:1 silicate clay minerals”. 1994, Volume 6.
- Rocha-Campos A.C., M.A. Basei, A.P. Nutman, Laura E. Kleiman, R. Varela, E. Llambias F.M. Canile, O. de C.R. da Rosa. 30 million years of Permian volcanism recorded in the Choiyoi igneous province (W Argentina) and their source for younger ash fall deposits in the Paraná Basin:SHRIMP U–Pb zircon geochronology evidence. Gondwana Research 19 (2011) 509–523
- Tak-Keun Oh , The effect of shear force on microstructure and mechanical property of epoxy/clay nanocomposites, Master Thesis at the University OF Florida 2004.
- Silva R. V., H. C. Ferreira Argilas bentoníticas: conceitos, estruturas, propriedades, usos, industriais, reservas, produção e produtores/fornecedores nacionais e internacionais Revista Eletrônica de Materiais e Processos, v.3.2 (2008) 26-35 ISSN 1809-8797

- Torres Sanchez, R.M., Lombardi, B.; Baschini, M.; Characterization of montmorillonites from bentonite deposits of north Patagonia, Argentina: Physicochemical and structural parameter correlation. The Journal of Argentine Chemical Society-vol.90-N` 4/6, 87-99 (2002).
- Sorption and Detoxification of Toxic Compounds by Bifunctional Organoclay, by Gerstl et al. (2004).
- VAN OLPHEN, H. e FRIPIAT, J.J.“Data Handbook for Clay Materials and other Non-Metallic Minerals”. Oxford: Pergamon Press, 1979.346p.
- Zev Gerstl, Ludmila Groisman, Chaim Rav-Acha, and Uri Mingelgrin Sorption and Detoxification of Toxic Compounds by Bifunctional Organoclay, J. Environ. Qual.